

CHALMERS



Modeling and compensation of a non-ideal I/Q-modulator

Master of Science Thesis

XIAOGENG XU
KAI WEN

Department of Signals and Systems
Division of Communication Systems
CHALMERS UNIVERSITY OF TECHNOLOGY
Göteborg, Sweden, 2007
Report No. EX083/2007

MODELING AND COMPENSATION OF A NON-IDEAL
I/Q-MODULATOR

By
Xiaogeng Xu, Kai Wen

SUBMITTED IN PARTIAL FULFILLMENT OF THE
REQUIREMENTS FOR THE DEGREE OF
MASTER OF SCIENCE
AT
CHALMERS UNIVERSITY OF TECHNOLOGY
GÖTEBORG, SWEDEN
SEPTEMBER 2007

© Copyright by Xiaogeng Xu, Kai Wen, 2007

CHALMERS UNIVERSITY OF TECHNOLOGY
DEPARTMENT OF
SIGNALS AND SYSTEMS
MICROTECHNOLOGY AND NANOSCIENCE

The undersigned hereby certify that they have read and recommend to the Faculty of Graduate Studies for acceptance a thesis entitled “**Modeling and Compensation of a Non-Ideal I/Q-Modulator**” by **Xiaogeng Xu, Kai Wen** in partial fulfillment of the requirements for the degree of **Master of Science**.

Dated: September 2007

Supervisor:

Christian Fager, Thomas Eriksson

Readers:

CHALMERS UNIVERSITY OF TECHNOLOGY

Date: **September 2007**

Author: **Xiaogeng Xu, Kai Wen**

Title: **Modeling and Compensation of a Non-Ideal
I/Q-Modulator**

Department: **Signals and Systems
Microtechnology and Nanoscience**

Degree: **M.Sc.** Convocation: **September** Year: **2007**

Permission is herewith granted to Chalmers University of Technology to circulate and to have copied for non-commercial purposes, at its discretion, the above title upon the request of individuals or institutions.

Signature of Author

THE AUTHOR ATTESTS THAT PERMISSION HAS BEEN OBTAINED FOR THE USE OF ANY COPYRIGHTED MATERIAL APPEARING IN THIS THESIS (OTHER THAN BRIEF EXCERPTS REQUIRING ONLY PROPER ACKNOWLEDGEMENT IN SCHOLARLY WRITING) AND THAT ALL SUCH USE IS CLEARLY ACKNOWLEDGED.

Table of Contents

Table of Contents	iv
List of Tables	vi
List of Figures	vii
Abstract	ix
Acknowledgements	x
1 I/Q Modulator Description	1
1.1 I/Q Modulator Structure	1
1.2 The Communication System with I/Q Modulation	3
1.2.1 The receiver	4
1.2.2 The demodulator	6
1.3 The Model Identification for Non-ideal I/Q Modulator	8
1.4 The compensation	9
2 Measurement System for Characterizing the I/Q Modulator	11
2.1 The Description of the Measurement System	11
2.2 Parameters Setting	14
2.2.1 The input signal	14
2.2.2 The power of transmitted signals	16
3 Signal Synchronization	18
3.1 Removing Delay	19
3.1.1 Resampling transmitted signal	19
3.1.2 Finding the integer delay	20
3.1.3 Finding the accurate non-integer delay	20

3.1.4	Removing delay and adjusting signal length	25
3.2	Normalizing	26
3.3	Averaging	27
3.4	Measurement Results	28
4	Modeling and Compensation for Linear Distortion	33
4.1	One Complex Channel Model and One Wiener Filter	34
4.2	One Complex Channel Model and Imbalance Problem	37
4.3	Two Complex Channel Model and Two Wiener Filters	41
4.4	Measurement Results Comparison	45
5	Modeling and Compensating for Nonlinear Distortion	48
5.1	Identification of Nonlinear Effects	48
5.2	Nonlinear Model	49
5.2.1	Memory and memoryless model	50
5.2.2	AM/AM and AM/PM model	51
5.3	Nonlinear Compensation	52
5.4	Measurement Results	54
5.4.1	Discussion on OSC's scaling setup	55
6	Pre-compensation	57
7	Conclusion	60
	Bibliography	62

List of Tables

2.1	The transmitted power corresponding to the available scaling	17
4.1	SNR comparison when input power is -21 dBm	46
5.1	Signal performances according to scaling	56

List of Figures

1.1	The structure of an I/Q modulator	2
1.2	Block Diagram of Communication System with I/Q modulator	3
1.3	The received signal in frequency domain	5
1.4	The structure of demodulator	6
1.5	The model identification procedure	9
1.6	The pre-compensation model for I/Q modulator	10
2.1	The connection of the equipments	12
2.2	The Electronic Signal Generator, Agilent E4438C	13
2.3	The Oscilloscope, Agilent Infiniium 54854A DSO	13
2.4	White Gaussian Noise as input signal, bandwidth $bw = 8\text{MHz}$, sample rate $f_{\text{ESG}} = 50\text{MHz}$, length $l = 20000$	15
3.1	Block diagram of the processes for signal synchronization	18
3.2	The delay between transmitted and received signals	21
3.3	Truncating the sinc function to limit the number of points introduces some problems in the resulting frequency response.	22
3.4	Magnitude of transmitted and received signal, transmitted signal power is -21dBm	29
3.5	SNR after removing integer delay	30
3.6	SNR after removing accurate delay	31
3.7	SNRs for different input power	32

4.1	Block diagram of channel model and Wiener filter for signal estimation	35
4.2	SNR after compensation by a complex Wiener filter	37
4.3	Block diagram of imbalance model and its compensation	38
4.4	I/Q imbalance model	38
4.5	SNR after compensation by a Wiener filter and imbalance matrix . .	40
4.6	Block diagram of complex I/Q channel model and compensation . . .	41
4.7	Two complex I/Q channel models	42
4.8	Detailed two complex I/Q channel model and compensation	43
4.9	SNR after compensation by two complex Wiener filters	44
4.10	SNR vs. Length of filters after linear compensation at -21 dBm . . .	45
4.11	SNR vs. Input power after linear compensation	46
5.1	Theoretical and measured power comparison for the input and output signal.	49
5.2	Nonlinear components within the system model	50
5.3	Block model for AM/AM and AM/PM envelope nonlinearity	51
5.4	Simplified One Nonlinearity–One Filter (Two-Box) Model	52
5.5	SNR after nonlinear compensation with different orders and signal power	54
5.6	SNR before and after nonlinear compensation	55
5.7	The OSC view of the received signal with input power $p = -5\text{dBm}$, three scaling settings.	56
6.1	Pre-compensation Progress	57
6.2	SNR with and without precompensation	58
6.3	SNR comparison	59

Abstract

Nowadays, I/Q modulators are widely utilized generating the source signals for wired and wireless communication system. Thus, a high quality of the I/Q modulator is especially crucial in order to assure high SNR at the receiver.

In this work, the tests were made with a 8MHz bandpass noise signal, which has statistical properties similar to modern communications signals. We firstly did identification for the system, and then used post- and pre-compensation to compensate for the non-idealities experienced in a practical I/Q modulator.

The post-compensation is used at the receiver side. There are two main techniques used in the post-compensation algorithm that we developed. First, a linear Wiener filter is used to compensate for the effects of imbalance and memory in the I/Q modulator. After that, the nonlinearity is compensated by a memoryless AM/AM polynomial. On the other hand, the pre-compensation is used at the transmitter side. While knowing the compensation filters' coefficients, pre-compensation can be applied to compensate any other signals before they are transmitted.

As for the results we achieved, SNR after linear compensation rises 6 dB to 45.5 dB, comparing with 39.5 dB without any compensation. Furthermore, nonlinear polynomial estimation improves the SNR to 48 dB. Using pre-distortion, the SNR at receiver reaches 44 dB.

Keywords: I/Q modulator, SNR, Wiener filter, imbalance, nonlinear, predistortion.

Acknowledgements

We would like to give our sincere gratitude to Christian Fager and Thomas Eriksson, our supervisors, for their suggestions and constant support during this research. Without their assistance, we could not finish this work smoothly.

We also would like to send our acknowledgements to Erik Ström, Tomas McKelvey, Irene Gu, for their lectures and tutorials during our early year studies in Digital Communications, Applied Signal Processing and Statistical Digital Signal Processing. This acknowledge also goes to all the lecturers and assistants in Programme of Digital Communication Systems and Technology.

The special thankfulness also goes to our parents in China, the encouragement and love from them is always essential to us.

Finally, we would like to give thanks to our friends in Sweden and all the people who helped us during this work.

Xiaogeng Xu, Kai Wen
Göteborg, September 2007

Chapter 1

I/Q Modulator Description

In this chapter, the I/Q modulator in a real communication system is introduced. The first section in this chapter shows the structure of the I/Q modulator, and analyzes the various interference presents. The second section describes the transmission system, and outlines the compensation procedure.

1.1 I/Q Modulator Structure

An I/Q modulator modulates two series of signals to the radio frequency (RF), with $\pi/2$ phase difference, which makes those two data orthogonal with respect to each other, and then combines them into one signal. The structure of I/Q modulator is as Figure 1.1:

y_{out} is the output signal from I/Q modulator. Assuming that the I/Q modulator is ideal,

$$y_{\text{out}} = A [I \cos(2\pi f_c) + Q \sin(2\pi f_c)] \quad (1.1.1)$$

where f_c is the RF frequency that the baseband signal is modulated to. $I + jQ$ is a discrete signal, while after Digital to Analog Converter (DAC), y_{out} is a continuous

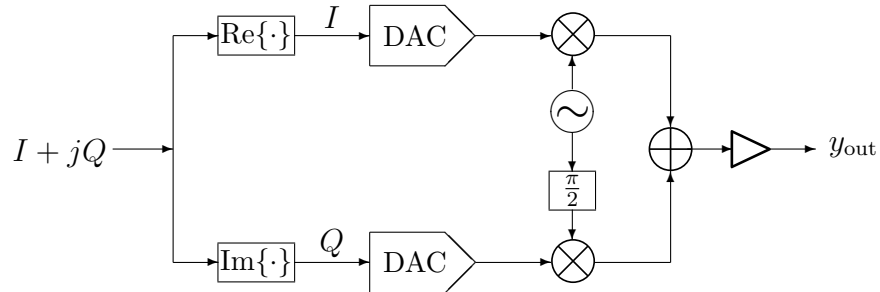


Figure 1.1: The structure of an I/Q modulator

signal.

However, in reality, I/Q modulators can never be completely described by Figure 1.1, since that none of the element inside is absolutely ideal. There is a list of effects that influence the I/Q modulator most. In this paper, the system model is identified, followed by the careful compensation solving the listed issues.

1. Channels for modulating I and Q signals respectively are not ideal. Even more, the impulse response of them are not balanced.
2. Phase difference between I and Q channels are not equal to 90° .
3. The amplifier is nonlinear especially at high output power.

Given the effects above, the first two items might cause channel non-ideality and crosstalk between I/Q channels, while the last item could make y_{out} nonlinear with respect to the I/Q input signals. Usually, there is another amplifier right after the I/Q modulator to provide enough power to transmit the y_{out} to a real channel, so that

the non-linearity of the signal is enlarged even more. All these modulator non-ideality contribute to degrade the quality of the signal at the receiver.

In reality, the y_{out} may be described by

$$y_{\text{out}} = L\{g_I * I \cos(2\pi f_c) + g_Q * Q \sin(2\pi f_c + \theta)\} \quad (1.1.2)$$

where $*$ is convolution, g_I and g_Q are the functions of I and Q channels in time domain. θ is a small angle error. L is the nonlinear function of the amplifier inside the I/Q modulator.

Equation 1.1.2 shows that, in reality, the output of the I/Q modulator is not a simple function, but with several unexpected effects and errors added.

1.2 The Communication System with I/Q Modulation

Having explained the structure of I/Q modulator above, this section introduces how it works in a communication system, and how the received signal could be demodulated to be two separate real signals.

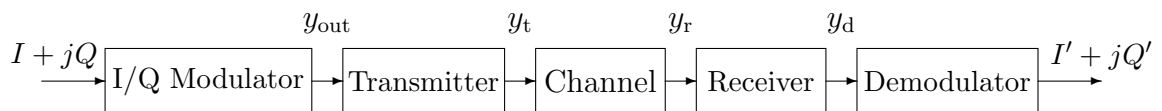


Figure 1.2: Block Diagram of Communication System with I/Q modulator

In Figure 1.2, y_{out} is fed to an RF transmitter, which controls the output power, then transmitted to the channel. The channel could be either wired or wireless. The

signal at the receiver can be expressed by

$$y_r = h_{\text{channel}} * y_t \quad (1.2.1)$$

where h_{channel} is a linear model for the channel between the transmitter and receiver.

1.2.1 The receiver

The receiver samples y_r with sampling frequency f_s . The sampling frequency is supposed to be calculated carefully in order to avoid aliasing effects. The sampling frequency should not be too high, otherwise, the amount of calculation is unnecessarily large. Here, an algorithm of calculating the sampling frequency at the receiver is utilized.

Reminding that, in general, the sampling frequency is supposed to fulfill the Nyquist Theorem,

$$f_s \geq 2bw \quad (1.2.2)$$

where bw is the bandwidth of the baseband signal.

Then after the signal is sampled to the carrier frequency f_c , a downconverter mixes it with a reference signal with intermediate frequency, and modulates it to the baseband.

However, in our special case, we are only interested in the bandwidth of $(f_c - bw, f_c + bw)$. Also, the noise floor out of the I/Q signal's bandwidth is low enough that not covering the concerned signal, we would like to introduce the following method, which could make the sampling procedure easier and clearer [5].

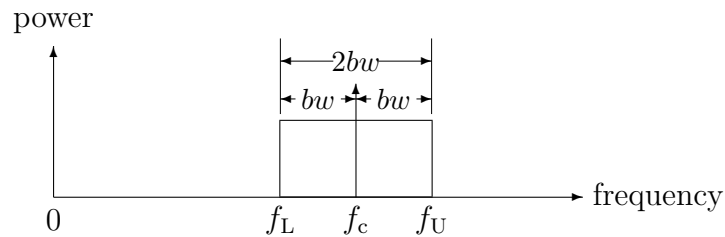


Figure 1.3: The received signal in frequency domain

In Figure 1.3, bw is the bandwidth of the I/Q data $I + jQ$. f_c is the carrier frequency that the I/Q data is modulated to.

$$f_L = f_c - bw$$

$$f_U = f_c + bw$$

The possible sample rates could be calculated by Equation 1.2.3

$$\frac{2f_U}{n} \leq f_s \leq \frac{2f_L}{n-1} \quad (1.2.3)$$

where n is the integer given by

$$1 \leq n \leq I_g \left[\frac{f_U}{bw} \right] \quad (1.2.4)$$

here $I_g \left[\frac{f_U}{bw} \right]$ means the integer part of the ratio $\frac{f_U}{bw}$.

Usually, there are more than one possible sample rate. The lowest sample rate should be larger than Nyquist rate, $f_s > 2bw$. For reducing the amount of calculation and memory requirements, the smallest f_s fulfilling the qualifications above is selected as the sample rate at the receiver. The Analog to Digital Converter (ADC) is also included inside the receiver. The output signal from the receiver y_d is a series of discrete real data.

1.2.2 The demodulator

The demodulator transforms the real signal y_d to two separate signals, I' and Q' .

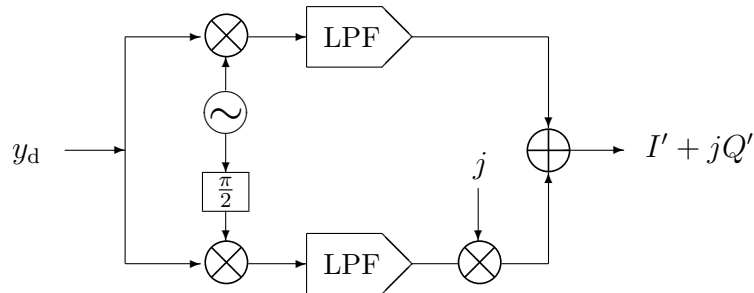


Figure 1.4: The structure of demodulator

As shown in Figure 1.4,

$$I' = f_{lp} * [y_d K \cos(2\pi f_c)]$$

$$Q' = f_{lp} * [y_d K \sin(2\pi f_c)]$$

where $*$ is the symbol of convolution, f_{lp} is a low pass filter, whose cutoff frequency is $2bw < f_{cutoff} < 2f_c$, where bw is the bandwidth of I . K is a constant to adjust the magnitude of the output signal.

Assuming that the whole system is ideal, while PA is linear, $h_{channel} = 1$, and the receiver does not cause any interference.

$$y_d = y_{out} = A(I \cos(2\pi f_c) + Q \sin(2\pi f_c)) \quad (1.2.5)$$

In order to reconstructing signal I , the demodulator does the following calculation:

$$\begin{aligned}
y_d \times K \cos(2\pi f_c) & \\
&= A(I \cos(2\pi f_c) + Q \sin(2\pi f_c)) \times K \cos(2\pi f_c) \\
&= K A I (\cos(2\pi f_c))^2 + K A Q \sin(2\pi f_c) \cos(2\pi f_c) \\
&= K \frac{1}{2} A I (\cos(4\pi f_c) + 1) + K \frac{1}{2} A Q \sin(4\pi f_c) \tag{1.2.6}
\end{aligned}$$

After going through the low pass filter,

$$I' = K \frac{1}{2} A I \tag{1.2.7}$$

Likewise,

$$\begin{aligned}
y_d \times K \sin(2\pi f_c) & \\
&= K \frac{1}{2} A I \sin(4\pi f_c) + K \frac{1}{2} A Q (1 - \cos(4\pi f_c)) \\
&\Rightarrow \text{Lowpass filter with cutoff frequency } f_{\text{cutoff}} \\
&= K \frac{1}{2} A Q \tag{1.2.8}
\end{aligned}$$

Here, $I' = I$ and $Q' = Q$, when $K = \frac{2}{A}$.

However, since that the communication system is not as ideal as we expected, the reconstructed signal $I' + jQ'$ is never exactly equal to $I + jQ$.

In practice, the process of signal transmission costs time, this small time period brings out a delay in the time domain, which is displayed through the received signal. What is more, the signal is attenuated, and noise is added at the receiver. Further, the channel imbalance and the amplifier's nonlinearity is enlarged and leads to the inaccurate of the received signal. Thus, $I' + jQ'$ is quite different from the original data, which results in the data loss, if not compensated for. Thus, the compensation is essential for accurately extracting the transmitted signal.

1.3 The Model Identification for Non-ideal I/Q Modulator

In order to improve the quality of the output signal from the I/Q modulator, the signal is going to be compensated according to a reasonable order. The essential step before compensation is the model identification. During this step, the characteristics of the I/Q modulator is characterized and quantified by measuring and processing a known signal. The signal is modulated by the I/Q modulator first and transmitted on a channel. After that, it is received and then processed by a computer. According to this consideration, the system that is going to be analyzed includes not only the I/Q modulator but also the channel and even the receiver. Consequently, we have to clarify that the model we derived is not the I/Q modulator only, instead, it is the whole measurement system. Thus, the compensation based on this model will improve the whole system. Since we used the good-quality channel and receiver to reduce the redundant interferences, the characteristics of the measurement system could mainly reflect to the I/Q modulator.

Assuming that, the I/Q modulator is a time-invariant device, its characteristic before model identification could be presented by a fixed function, which is derived from the comparison between $I + jQ$ and $I' + jQ'$, see Figure 1.2. To make it simple, let $x(n) = I + jQ$, $y(n) = I' + jQ'$, and the improved data after compensation is named $\hat{x}(n)$.

There are three main effects needed to remove before model identification: the delay, the fading and the added noise. Only if these three are solved perfectly, the signal is reflecting the performance of the I/Q modulator(and the receiver), which

consists of both the linear and nonlinear characteristics. Figure 1.5 outlines the procedure used for the model identification.

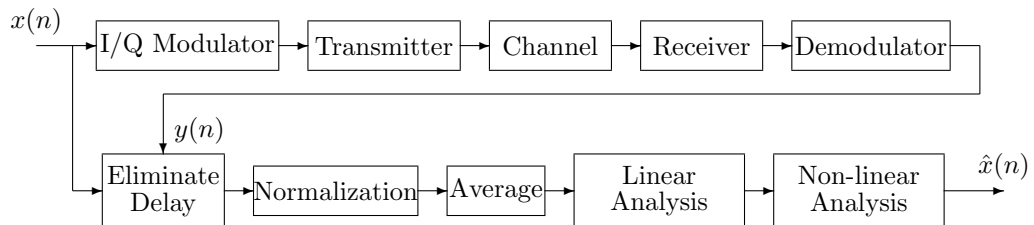


Figure 1.5: The model identification procedure

According to Figure 1.5, 'Eliminate Delay' is set as the first step after receiving $y(n)$, because every following procedure is based on a precondition, that $y(n)$ is supposed to be synchronized to $x(n)$. Having eliminated the delay, we use a complex variable to adjust the power and phase shift during the transmission. 'Average' is used to remove the influences from the white noise and quantization error. However, it could not be used in a real communication system, since that, mostly, it is impossible or inefficient to transmit the same signal several times just for averaging. So far, the preparation is finished for the compensations. Linear and non-linear compensations are the most important procedures to reconstruct the I/Q data. They will be introduced in details separately in the following chapters.

1.4 The compensation

From the model identification, the characteristics of the I/Q modulator are derived and reserved as the parameters for the linear and nonlinear compensations. As discussed before, the pre-compensation is more convenient and accurate for the further

signal transmission. The flow chart of pre-compensation is shown as Figure 1.6.

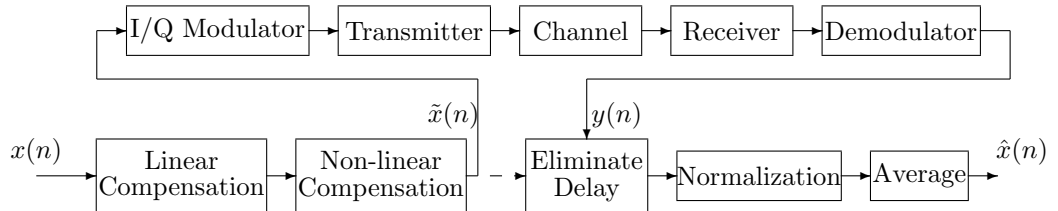


Figure 1.6: The pre-compensation model for I/Q modulator

Where the dash line in this figure does not appear in reality. When transmitting a signal, the receiver could not know the transmitted signal, therefore, the delay could not be eliminated in this way. According to our problem, the known signal is still used to remove the delay. So that we could distinguish the performance of the compensation clearly.

As described in Figure 1.6, $x(n)$ is compensated before transmitted, which is the final model that used in a real transmission system. While the pre-compensation blocks are working for the unique I/Q modulator, they could help to restore the I/Q data from the non-ideal I/Q modulator.

Chapter 2

Measurement System for Characterizing the I/Q Modulator

A measurement system is designed for characterizing the I/Q modulator. Every instrument in this model has to be as ideal as possible in order to add minimum distortion to the measured signal. They are supposed to be both linear and time-invariant. Besides, all the effects which is not caused by the I/Q modulator should be fixed by careful design. The measurement system has a simple structure comparing with real communication systems. However, it could provide a legible outline to test how the compensation methods improve the performance of I/Q modulator. The structure of the system is introduced first. The signal utilized for the modulator characterization is presented, as well.

2.1 The Description of the Measurement System

In a practical communication system, there are several factors affecting the received signal. However, to make the system simple and reflect the characteristics of the I/Q modulator clearly, the designed model should avoid those effects as much as possible.

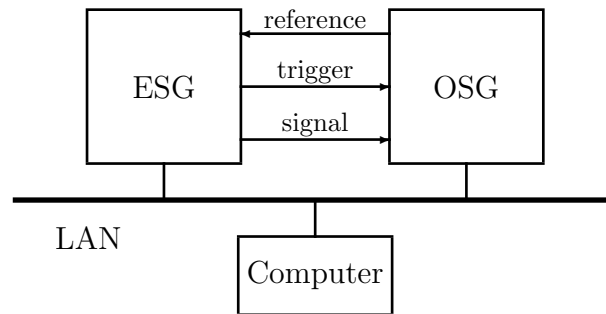


Figure 2.1: The connection of the equipments

Also, the system is supposed to be highly efficient and intuitive. The system is designed to be a wired communication system, which is composed of a computer, an Electronic Signal Generator (ESG), and an Oscilloscope (OSC). All of them are connecting to a Local Area Network (LAN). Figure 2.1 shows the system and how the equipments connect to each other.

The computer works as a baseband signal generator, which provides two series of data. It sends the data to the ESG through the LAN. Also, after being received by the OSC, the data is delivered to the computer again. All signal processing, including modulator model identification and pre-compensation is done in the computer.

The ESG works as both I/Q modulator and transmitter. It receives the baseband signal from the computer, modulates it to a Radio Frequency (RF) I/Q signal. The ESG also amplifies the signal to a certain power, which is set by the user, then sends the signal to the channel. Besides the I/Q data, the ESG transmits a trigger as well. It is very important to have a trigger transmitted with the I/Q data, so that the receiver could detect the correct time to start reading the signals. In this model, the ESG is Agilent E4438C, see Figure 2.2.

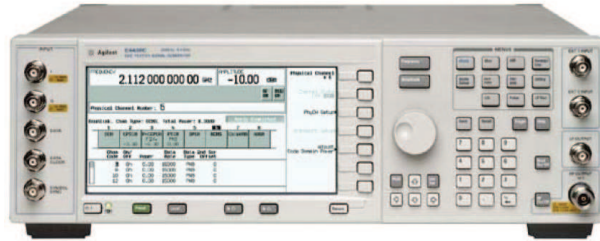


Figure 2.2: The Electronic Signal Generator, Agilent E4438C

The OSC is an accurate instruments, which receives wide band signals, and presents it on its monitor. Different from the ESG, the OSC doesn't perform demodulation, it is only a receiver. In the experiment, the signal is demodulated by the computer. Figure 2.3 is the the picture of Agilent Infiniium 54854A DSO, the OSC used in the system.



Figure 2.3: The Oscilloscope, Agilent Infiniium 54854A DSO

In real communication systems, there are no synchronizing connections between

transmitters and receivers. The devices use their own crystal to generate a signal with the reference frequency then convert them to the desired frequencies. But, no two crystals could generate signals with exactly the same frequency. The frequency drift is not neglectable at the receiver. In our test case, we add a reference connection between the ESG and the OSC to avoid synchronization problems. A 10MHz signal is generated by the OSC, and fed to the ESG by a cable. In this way, both the ESG and the OSC are using the same reference frequency. Although, there is no guarantee that the frequency transformed from the reference are absolutely the same, the error is decreased by this setup.

2.2 Parameters Setting

Figure 2.1 presents the whole measurement system used for the experiment. Several parameters are supposed to be defined before the measurement starts. We decided to simulate a signal generator for Wideband Code Division Multiple Access (W-CDMA) technique of 3G cellular network. The carrier frequency of W-CDMA is from 2.1GHz to 2.2GHz. Here, we select $f_c = 2.14\text{GHz}$.

2.2.1 The input signal

Band-limited white noise is widely used to test the frequency response of a certain channel or an instrument. Because the magnitude of the signal is flat inside the band statistically, the white noise could reflect the characteristics of the device under test very well. For the input signal, two series of independent low-pass white noise are therefore generated by the computer as the real and imaginary components of I/Q

data, respectively. The bandwidth of the input signal is selected to be $bw = 8\text{MHz}$.

Usually, the signal is upsampled before it is treated by the modulator in order to extract enough information and avoid aliasing. The sample rate should be at least twice of the highest frequency of the sampled signal, which is the Nyquist Theorem. The modulator sample rate is denoted as $f_{\text{ESG}} = 50\text{MHz}$. In order to make sure that the signal is sampled accurately, the upsampling is done by the computer before uploading the data to the ESG.

In this case, the output signal sent from the computer is a complex baseband white noise, with bandwidth 8MHz , sample rate 50MHz , and length $l = 20000$. This signal is defined as the baseband I/Q data $x(n)$ in the following chapters. It is shown in Figure 2.4.

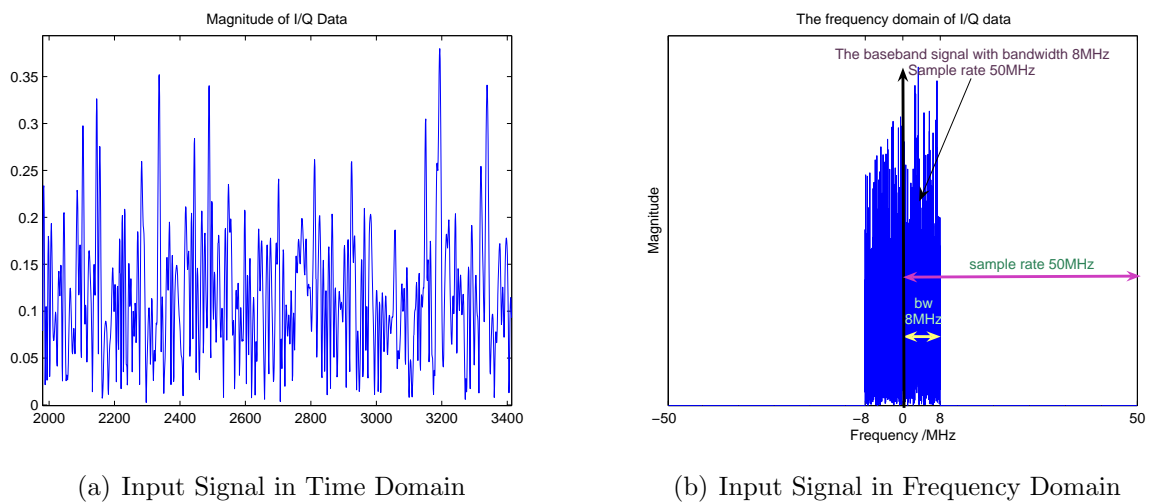


Figure 2.4: White Gaussian Noise as input signal, bandwidth $bw = 8\text{MHz}$, sample rate $f_{\text{ESG}} = 50\text{MHz}$, length $l = 20000$.

At the OSC, the I/Q data is sampled by f_s and presented on the monitor. The formula of calculating the sample frequency is mentioned previously in Chapter 1, see

Equation 1.2.3 and 1.2.4. Since only a fixed set of OSC sample rates are available, we selected $f_s = 200\text{MHz}$.

2.2.2 The power of transmitted signals

In order to fully characterize the performance of the I/Q modulator, the signal is supposed to be transmitted at several power levels. Different from a practical receiver, an oscilloscope works as a receiver in our system. However, the accuracy of the digitized signal depends on the amplitude scaling setting. The received signal is supposed to fill the monitor without or with very little clipping. When changing the signal's power, the scaling of the OSC should therefore be adjusted accordingly.

By the practical limitations of the OSC, there are only finite set of discrete scaling selections available. To make the signal fill the monitor, the transmitted power is supposed to be calculated depending on the scalings. We use the following method to decide the transmitted powers. First, fix the scaling, for instance, $S_0 = 100 \text{ mV/grid}$. Then adjust the transmitted power $P_0 \text{ mW}$, to make the signal fill the screen of the OSC. Next, switch to another scaling $S_1 \text{ mV/grid}$, use the Equation 2.2.1 to calculate the proper transmitted power $P_1 \text{ mW}$.

$$\frac{P_1}{P_0} = \frac{S_1^2}{S_0^2} \quad (2.2.1)$$

Another power unit is used to set the transmitted power at the ESG, which is called dBm. It represents a measured power level in dB (decibel) relative to 1 mW

(milli-Watt). To express an arbitrary power P mW to p dBm,

$$p = 10 \log_{10} P \quad (2.2.2)$$

where P is in mW.

From Equation 2.2.1, Equation 2.2.2 becomes

$$p_1 = p_0 + 20 \log_{10} \frac{S_1}{S_0} \quad (2.2.3)$$

where p_1 and p_0 are in dBm.

After calculation, the Table 2.1 presents the transmitted powers, according to different scalings.

Table 2.1: The transmitted power corresponding to the available scaling

Num.	1	2	3	4	5	6	7
Scaling (mV/grid)	500	200	100	50	20	10	5
Transmitted power(dBm)	7	-1	-7	-13	-21	-27	-33

Notice that there is an assumption made for Equation 2.2.1 and 2.2.3: the power of the noise has to be small compared to the power of the signal. Otherwise, Equation 2.2.1 becomes

$$\frac{P_1 + P_N}{P_0 + P_N} = \frac{S_1^2}{S_0^2} \quad (2.2.4)$$

when P_N is not neglectable, P_1 and P_0 are not linear anymore.

Chapter 3

Signal Synchronization

When the signal is received, we need to compare it with transmitted signal to identify the modulator model. But through the analog channel, the signal has been rotated, delayed, phase-shifted and amplified, also the noise has been added to the signal.

Therefore, before modeling and compensating the modulator, the first step in the system model identification is to synchronize the received and transmitted signals. This means that the delay, phase shifts and amplitude levels in received signal need to be identified and eliminated. In this chapter, we will focus on this pre-processing of the received signal, hereafter denoted signal synchronization.

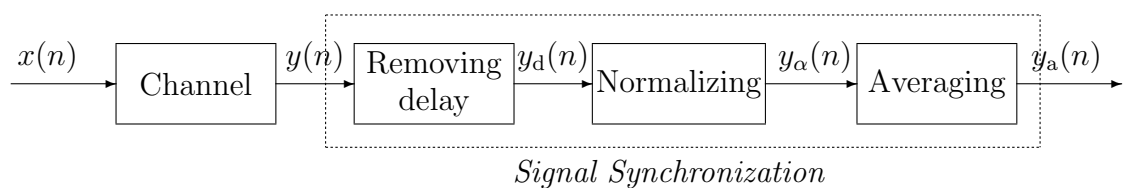


Figure 3.1: Block diagram of the processes for signal synchronization

As shown in the Figure 3.1, the signal synchronization includes removing delay to eliminate the accurate delay from received signal, normalizing to find a complex constant to adjust the received signal's power and constant phase shift, averaging several

groups of received signal to decrease the effects of zero-mean noises from the channel. After these treatments, a direct comparison between received and transmitted signal becomes possible.

3.1 Removing Delay

In a general sense, delay refers to a lapse of time that is required for a signal to travel from the transmitter to the receiver. It is always inevitable in real transmission channels, and needs to be removed before the signal is parsed. The first task of synchronization is therefore to determine and remove the delay in the received signal.

3.1.1 Resampling transmitted signal

In order to recover the signal more accurately, the sampling frequency we have used at the receiver is normally several times higher than that at the transmitter. Thus, the transmitted and received signals have different length. To find the delay, first they must be synchronized to have the same sample rate.

There are two ways to achieve the goal, upsampling the shorter signal or down-sampling the longer one. We prefer upsampling since all the original samples are expected to be retained to obtain an accurate result in the further processing.

Let L denote the resampling factor, the sequence in received signal vector is re-sampled at L times the original sampling rate, using the resampling implementation. An anti-aliasing lowpass FIR filter is also applied to the signal vector during the re-sampling process. After resampling, the received and transmitted signals now have the same sample rate.

3.1.2 Finding the integer delay

When the sampling frequency is high enough and the transmitted and received signals have same sample rate, a common method of finding the delay is to calculate the cross correlation between the transmitted signal $x(n)$ and the received signal $y(n)$.

$$r_{xy}(k) = E\{x(n)y^*(n-k)\} \quad (3.1.1)$$

Here since an expectation cannot be computed in real implementation, we estimated the correlation by summing. For discrete-time signals, the maximum correlation corresponds to the closest integer delay d_i . When $r_{xy}(k)$ reaches its maximum value, the value of integer delay d_i is obtained that $d_i = k$ samples.

As an example from experiment, the waveforms of the received and transmitted signal are normally as below in Figure 3.2, where the delay obviously exists between them.

When the integer delay is determined, it is easy to remove from the signal sequence. The received signal after removing the integer delay d_i is called $y_i(n)$,

$$y_i(n) = y(n + d_i) \quad (3.1.2)$$

3.1.3 Finding the accurate non-integer delay

Although the transmitted signal $x(n)$ and the received signal $y(n)$ are discrete, all the data in the transmission system is converted into analog data. There is no guarantee that the delay in the received signal is integer. Generally, after converting back into digital signal at the receiver, the delay in $y(n)$ is not an integer value. The task in

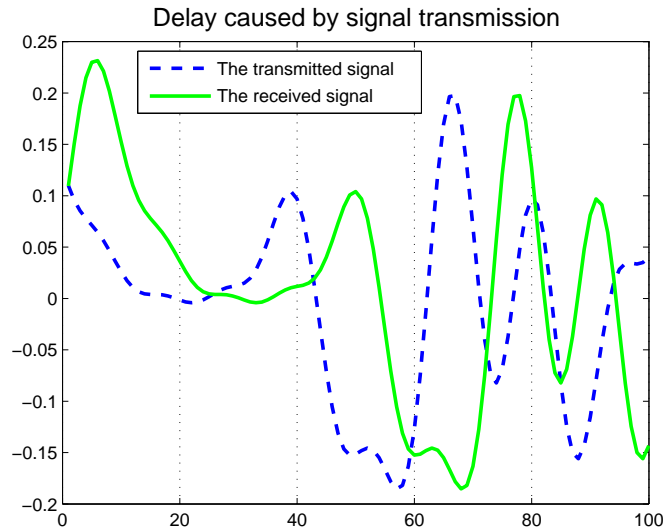


Figure 3.2: The delay between transmitted and received signals

this subsection is therefore to find out the accurate non-integer delay in the received signal.

Given the integer delay d_i , the accurate non-integer delay d_a should be a real value in the interval $(d_i - 0.5, d_i + 0.5)$.

Now we have the signal $y_i(n)$ that has already removed integer delay d_i , in order to find the non-integer delay d_a , one way is to restore the discrete-time signal $y_i(n)$ to the continuous-time signal $y_i(t)$ by using a method called *sinc interpolation*. The formula is presented as below

$$\begin{aligned}
 y_i(t) &= \sum_{k=1}^N y_i(kT) \text{sinc}((t - kT)/T) \\
 &= \sum_{k=1}^N y_i(kT) \frac{\sin(\pi(t - kT)/T)}{\pi(t - kT)/T}
 \end{aligned} \tag{3.1.3}$$

where $y_i(nT) = y_i(n)$ is regarded as the uniformly spaced samples of a bandlimited

continuous-time signal $y_i(t)$, N is the length of $y_i(n)$, and T is the sampling period.

We involved the sinc function because it is an ideal low-pass filter that could principally recover the signal without distortion. However, the sinc function can not be achieved in reality since it has infinite length in the time domain. In real implementations, simply truncating the sinc function to limit the number of points, using a square window, would introduce some problems in the resulting frequency response, shown in Figure 3.3. [4]

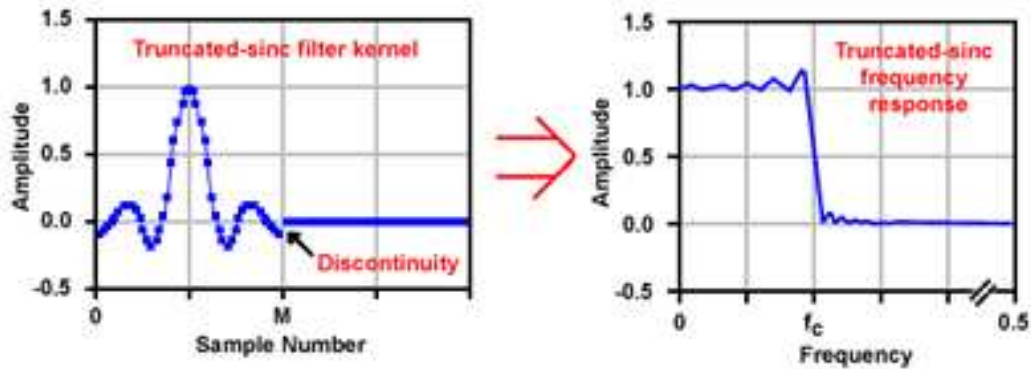


Figure 3.3: Truncating the sinc function to limit the number of points introduces some problems in the resulting frequency response.

As displayed in the figure, the discontinuity in the impulse response causes ripple in the passband and reduces stopband attenuation. To solve this problem, a windowed-sinc filter including the sinc function and a smoothly tapered window function is used.

A variety of such window functions are possible, here the Hanning window of length 65 is applied to truncate the sinc impulse response. The Hanning window is

defined as

$$Hanning_{65}(n) = \frac{1}{2} \left[1 - \cos\left(\frac{2\pi n}{N+1}\right) \right] \quad (3.1.4)$$

This window does a good job of forcing the ends of sinc function to zero, resulting in a much smoother frequency response. Thus, it does not show obvious sidelobes in frequency domain, therefore has less spectrum distortion comparing with a square window.

When the reconstruction filter has been chosen, the Equation 3.1.3 is converted to

$$y_i(t) = \sum_{k=1}^N y_i(kT) [\text{sinc}((t - kT)/T) \cdot Hanning_{65}(t - kT)/T] \quad (3.1.5)$$

where N and T is as same as defined before. In this way, the discrete signal $y_i(n)$ has its continuous form $y_i(t)$.

In principle, when we have the continuous signal $y_i(t)$, we could sample it again to get a shifted signal $y_i(n + \Delta)$, where Δ is a real value between -0.5 and $+0.5$. Then the Δ , that causes the maximum crosscorrelation between $y_i(n + \Delta)$ and $x(n)$, should be the difference between the integer and the accurate delay we need to find. Here $y_i(n + \Delta)$ has the same sampling period T as $y_i(n)$, but has been shifted Δ samples. In a real implementation, $y_i(n + \Delta)$ could be generated directly from the discrete signal $y_i(n)$ by using sinc interpolation, as described below

$$\begin{aligned} y_i(n + \Delta) &= \sum_{k=1}^N y_i(k) [\text{sinc}(n + \Delta - k) \cdot Hanning_{65}(n + \Delta - k)] \\ &= \mathbf{Y}_i * \mathbf{h}(\Delta) \quad n = 0, 1, \dots, N \end{aligned} \quad (3.1.6)$$

where

$$\begin{aligned}\mathbf{Y}_i &= y_i(n) = y(n + d_i) \\ \mathbf{h}(\Delta) &= \text{sinc}(n + \Delta) \cdot \text{Hanning}_{65}(n + \Delta)\end{aligned}\quad (3.1.7)$$

where N is the length of $y_i(n)$, and “ \cdot ” denotes multiply. This process is same as filtering the signal \mathbf{Y}_i through a windowed-sinc filter $\mathbf{h}(\Delta)$.

In this way, by trying different Δ in the interval $(-0.5, 0.5)$, we could find a Δ_m that causes the maximum crosscorrelation between the shifted signal $y_i(n + \Delta_m)$ and the transmitted signal $x(n)$. Because Δ_m is the difference between d_i and d_a , we know the accurate delay d_a

$$d_a = d_i + \Delta_m \quad (3.1.8)$$

which is a non-integer value between $d_i - 0.5$ and $d_i + 0.5$.

For efficiency, we do not need to shift $y_i(n)$ then calculate the crosscorrelation in real implementation, but shift the crosscorrelation between $x(n)$ and $y_i(n)$ directly. The crosscorrelation is described as

$$r_{xy_i}(k) = E\{x(n)y_i^*(n - k)\} \quad (3.1.9)$$

Correspondingly, Equation (3.1.6) should be converted to

$$\begin{aligned}r_{xy_i}(n + \Delta) &= \sum_{k=-\infty}^{\infty} r_{xy_i}(k) [\text{sinc}(n + \Delta - k) \cdot \text{Hanning}_{65}(n + \Delta - k)] \\ &= \mathbf{r}_{xy_i} * \mathbf{h}(\Delta)\end{aligned}\quad (3.1.10)$$

The same as above, trying different Δ , the one that yields the highest maximum $r_{xy_i}(n + \Delta)$ would be the exact Δ_m we found. The accurate delay is also as described in Equation (3.1.8).

3.1.4 Removing delay and adjusting signal length

Since the delay might not be an integer value, it could not be eliminated by directly removing the initial samples in the received signal. Instead, sinc interpolation is utilized again.

The received signal after removing the accurate delay d_a is called $y_d(n)$,

$$y_d(n) = y(n + d_a) = y(n + d_i + \Delta_m) = y_i(n + \Delta_m) \quad (3.1.11)$$

therefore we denote $y_d(n)$ is the shifted version of $y_i(n)$. We already know the value of Δ_m which is the difference between d_a and d_i , it is easy to shift $y_i(n)$ to $y_i(n + \Delta_m)$ by using sinc interpolation,

$$\begin{aligned} y_d(n) &= y_i(n + \Delta_m) \\ &= \sum_{k=1}^N y_i(k) [\text{sinc}(n + \Delta_m - k) \cdot \text{Hanning}_{65}(n + \Delta_m - k)] \\ &= \mathbf{Y}_i * \mathbf{h}(\Delta_m) \end{aligned} \quad (3.1.12)$$

where

$$\begin{aligned} \mathbf{Y}_i &= y_i(n) = y(n + d_i) \\ \mathbf{h}(\Delta_m) &= \text{sinc}(n + \Delta_m) \cdot \text{Hanning}_{65}(n + \Delta_m) \end{aligned} \quad (3.1.13)$$

Again, $y_d(n)$ can be presented as the convolution between the signal after removing integer delay and an windowed-sinc function about Δ_m .

By now, $y_d(n)$ is the received signal that has already removed accurate delay, and it will be used for further analysis.

Finally, if the transmitted signal is L samples long, the received signal after removing delay will have $L - d_i$ samples. In order to adjust them to be the same length, the redundant d_i samples at the end of the transmitted signal are discarded.

3.2 Normalizing

After amplifiers and channel, the amplitude and phase offset of signal, which are affected by noise and fading, have been changed. Normalizing therefore is the procedure to normalize the amplitude and constant phase offset of the received signal. The goal of this step is to find a value of the complex constant α , where $\alpha = \alpha_I + j\alpha_Q$, to minimize the mean squared error (MMSE) between $x(n)$ and $y_d(n)$, and make it possible to directly compare the transmitted and received signals side-by-side.

$$\begin{aligned}
\|x - \alpha y_d\|^2 &= (x - \alpha y_d)^H (x - \alpha y_d) \\
&= x^H x + \alpha^* \alpha y_d^H y_d - \alpha^* y_d^H x - \alpha x^H y_d \\
&= x^H x + (\alpha_R - j\alpha_I)(\alpha_R + j\alpha_I) y_d^H y_d - (\alpha_R - j\alpha_I) y_d^H x - (\alpha_R + j\alpha_I) x^H y_d \\
&= x^H x + (\alpha_R^2 + \alpha_I^2) \|y_d\|^2 - (\alpha_R - j\alpha_I) y_d^H x - (\alpha_R + j\alpha_I) x^H y_d \quad (3.2.1)
\end{aligned}$$

We find the derivative with respect to α_R and α_I , and set them to zero:

$$\begin{aligned}
\frac{\partial \|x - \alpha y_d\|^2}{\partial \alpha_R} &= 2\alpha_R \|y_d\|^2 - y_d^H x - x^H y_d = 2\alpha_R \|y_d\|^2 - 2\text{Re}\{y_d^H x\} = 0 \\
\Rightarrow \alpha_R &= \frac{\text{Re}\{y_d^H x\}}{\|y_d\|^2} \quad (3.2.2)
\end{aligned}$$

and

$$\begin{aligned}
\frac{\partial \|x - \alpha y_d\|^2}{\partial \alpha_I} &= 2\alpha_I \|y_d\|^2 + j y_d^H x - j x^H y_d = 2\alpha_I \|y_d\|^2 - 2\text{Im}\{y_d^H x\} = 0 \\
\Rightarrow \alpha_I &= \frac{\text{Im}\{y_d^H x\}}{\|y_d\|^2} \quad (3.2.3)
\end{aligned}$$

Finally we get

$$\alpha = \alpha_{\text{R}} + j\alpha_{\text{I}} = \frac{\text{Re}\{y_{\text{d}}^H x\} + j\text{Im}\{y_{\text{d}}^H x\}}{\|y_{\text{d}}\|^2} = \frac{y_{\text{d}}^H x}{\|y_{\text{d}}\|^2} \quad (3.2.4)$$

From Equation (3.2.4), the complex α that minimizes the power of the error is found. Thus, α both corrects amplitude differences and compensates for residual phase differences.

The received signal normalized by α is

$$y_{\alpha}(n) = \alpha y_{\text{d}}(n) \quad (3.2.5)$$

By now, we have assured that $x(n)$ and $y_{\alpha}(n)$ have normalized amplitude and no phase offset.

3.3 Averaging

The purpose of averaging is to reduce the affect of zero-mean white noise from channel and quantization error from the A/D converter in the oscilloscope.

At the receiver, we received several groups of data. After removing delay and normalizing amplitude and phase for each group, they could be averaged for each sampling instant. Assume the M groups of signal after normalizing are called $y_{\alpha 1}(n)$, $y_{\alpha 2}(n)$, \dots , $y_{\alpha M}(n)$, the averaged signal therefore is

$$\bar{y}_{\alpha}(n) = \frac{1}{M} \sum_{k=1}^M y_{\alpha k}(n), \quad n = 1, 2, \dots, N \quad (3.3.1)$$

where M is the number of measurements, and N is the length of $y_{\alpha}(n)$.

Although averaging is really not possible to be done in a real system, we introduced it here to make sure that the modeling of the modulator is more accurate in the

following step. Because only if the output signals are less affected by the unwanted white noise or quantization error, the modulator model we find could be more reliable and then the compensation for the modulator could be more effective.

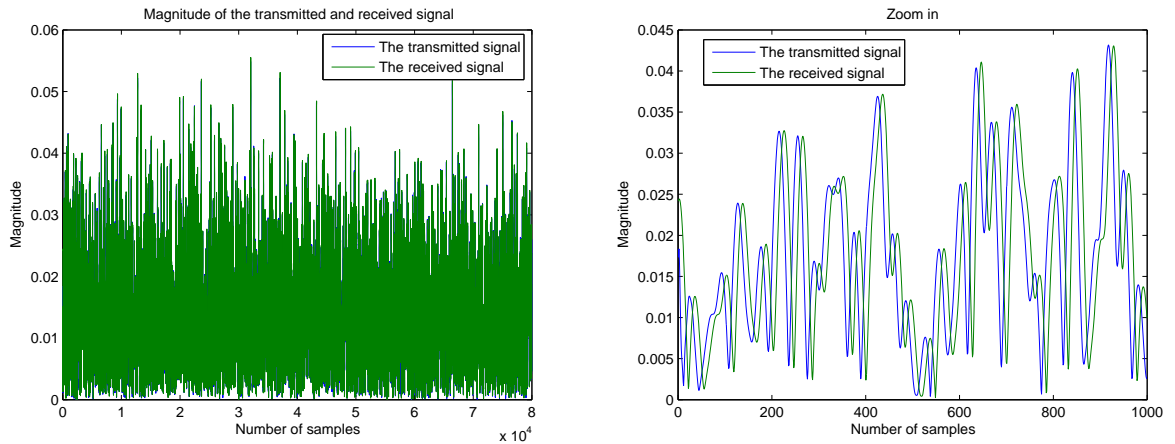
3.4 Measurement Results

Since comparing the received and transmitted signals is only possible after they are synchronized, we put the measurement results at the last section of this chapter. The results we get here are from the signals that have been processed by removing delay, normalizing and averaging.

Before synchronization, the magnitude of transmitted and received signal when the transmitted power is -21 dBm are shown in Figure 3.4. We chose -21 dBm to guarantee that the input power is in the linear phase of the modulator. As displayed in the Figure 3.4, the magnitude of transmitted and received signals looks similar because the channel is almost ideal, but the delay in the received signal is obvious.

After synchronization, we can compare the received and transmitted signal. The SNR (Signal-to-Noise Ratio) is widely used to compare the level of a desired signal to the level of background noise. The higher the ratio, the less obtrusive the background noise is. Instead of the real background noise, the noise in this case is the difference between desired signal $x(n)$ and output signal $y'(n)$, $y'(n)$ could be the output from any compensation stages. So the SNR here indicates the degree of similarity between $x(n)$ and $y'(n)$: the higher the ratio, the more similar they are. The definition of SNR is

$$\text{SNR}[\text{dB}] = 10 \log_{10} \left(\frac{P_{x(n)}}{P_{x(n)-y'(n)}} \right) \quad (3.4.1)$$



(a) Magnitude of transmitted and received signal

(b) Zoom in of (a)

Figure 3.4: Magnitude of transmitted and received signal, transmitted signal power is -21dBm.

where P is average power of the signal. For a certain transmitted signal $x(n)$, the value of SNR only depends on the output signal $y'(n)$, so we will focus on the improvement of $y'(n)$ to achieve an improvement of the SNR.

We calculated the SNRs for two groups of output signals, that is the received signal after removing integer delay and after removing accurate delay.

First, by just removing the integer delay from the received signals, the SNRs are calculated and shown in Figure 3.5. The blue points are the SNRs before averaging for 50 measurements respectively. The green curve show the SNRs after averaging, which increase following the number of measurements involved in averaging.

As the DC component is eliminated from signal before every process, the added noise from channel is considered as zero-mean white noise. Thus, the SNRs before averaging are randomly distributed, approximately ranging from 28 dB to 35 dB. After averaging, the performance is gradually improved. The SNRs after averaging

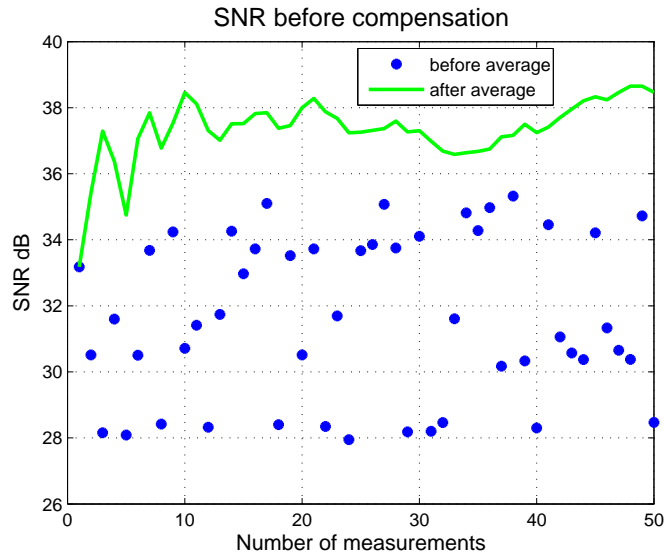


Figure 3.5: SNR after removing integer delay

fluctuate around 38 dB, reaching a peak at 38.5 dB when all 50 measurements are involved in averaging.

Then for the same received signal, we determined and removed the accurate delay using sinc interpolation mentioned in Section 3.1.3, and calculated the SNRs, shown in Figure 3.6.

At a glance, it is obvious the performance is better than that in Figure 3.5. Before averaging, the SNRs for each measurement are slightly higher than just removing integer delay, ranging from 33 dB to 36 dB. While after averaging more and more number of measurements, the SNRs are also increasing but much more smoother, reaching a peak at 39.4 dB by averaging all 50 groups of signals. Therefore, although the difference between integer delay and accurate delay is small, it can not be ignored.

From the previous discussion, we chose a certain transmitted power -21 dBm as

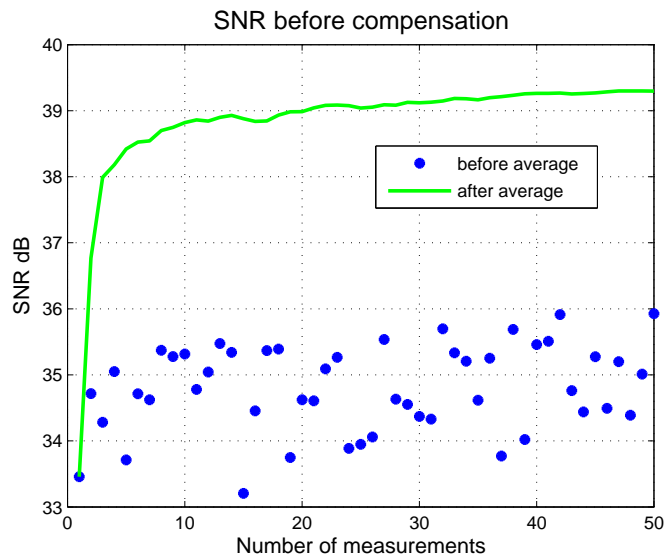


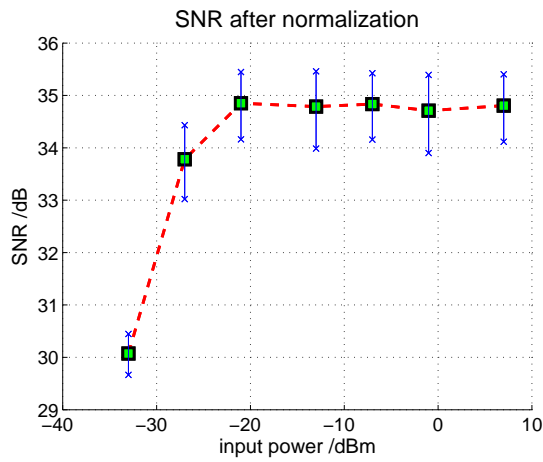
Figure 3.6: SNR after removing accurate delay

an example to show that the SNRs increase with the number of measurements for averaging. Now to present the measurement results in a general case, we will calculate the SNRs for different transmitted power ranging from -35 dBm to 10 dBm, in the display range of the oscilloscope. By considering the scaling of OSC which will be discussed in Section 2.2.2, 7 transmitted powers have been chosen in our experiment, they are -33 dBm, -27 dBm, -21 dBm, -13 dBm, -7 dBm, -1 dBm and 7 dBm. We chose them to assure that the quantization errors in OSC for these powers are almost same, therefore the results are achieved under the same hardware condition, which make them equal to be compared.

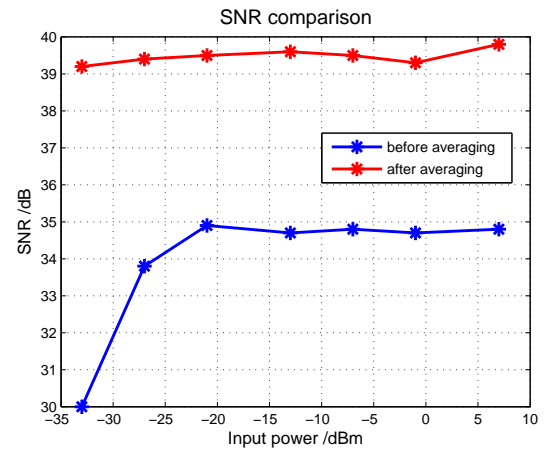
Before averaging, to have a general idea about the distribution of SNRs for 50 groups of received signal, Figure 3.7a displays the range of SNRs for different transmitted powers. The blue lines are the range of SNRs and the green points are the

averaged values of SNRs on the certain powers.

As a comparison, Figure 3.7b shows the SNRs before and after averaging corresponding to different transmitted powers. From the figure, the SNRs after averaging for most transmitted powers reaches 39.5 dB, which are improved more than 4 dB comparing with that before averaging. What is worth to mention is that when the transmitted power is below -25 dBm, the SNRs before averaging is low because the signals are dominated by noise.



(a) Range of SNR vs. Input power



(b) SNR before and after averaging

Figure 3.7: SNRs for different input power

Chapter 4

Modeling and Compensation for Linear Distortion

Having synchronized the transmitted and received signals, it is possible to compare them in order to determine a model of the I/Q modulator, and subsequently compensate its non-ideal characteristics. This chapter focuses on linear compensation, while the next chapter will introduce signal recovery from nonlinear distortion.

In this chapter, three linear compensation models are presented in order of enhancing the simulation accuracy. The first one is a complex Wiener filter. A Wiener filter is a commonly used linear, discrete-time filter to estimate random signals. A complex Wiener filter with proper length could compensate the linear distortion of a certain channel.

When we use Wiener filter to estimate signals, we assume that the I/Q modulator has two independent parallel channels for I and Q signal respectively. However, in practice, the analog quadrature modulator, which is used to modulate the I/Q data

to RF, can not generate quadrature carriers that have exactly the same amplitudes and an exact phase difference of 90 degrees. This non-ideal effect is called gain/phase imbalance and causes cross-talk between the I and Q channels. Moreover, the leakage of the carrier to the transmitted signal can cause a DC offset in the demodulated received signal, but as we have gotten rid of the DC part before compensation, the DC offset does not dominate the distortion, and will not be mentioned in the following compensation methods.

So the next two compensation methods in this chapter will consider this modulator imbalance problem. The second method for linear compensation has an imbalance matrix with length equals one after the Wiener filter. The imbalance coefficients between I and Q channels after Wiener filter is calculated and used to compensate the system as an additional step.

Instead of deriving the Wiener filter and cross matrix in two separate steps, it is more efficient and advanced to combine them into one stage by using two complex Wiener filters. This idea is introduced in the third section.

4.1 One Complex Channal Model and One Wiener Filter

Wiener filtering is used for linear compensation of the system channel in our project. This section will present the process of modeling the system channel and designing a causal FIR Wiener filter.

In digital signal processing, it is important to estimate signals from noise-corrupted measurements. The goal is to design an optimal linear filter $G(z)$ such that the output

of the filter is the “best” estimation of the desired signal under Mean Square Error (MSE) criterion.

A Wiener filter is an optimal digital linear filter which is used for signal estimation under the MSE criterion. Figure 4.1 shows the block diagram of channel model and signal estimation with a Wiener filter [2]. Here the channel block includes the I/Q modulator as well.

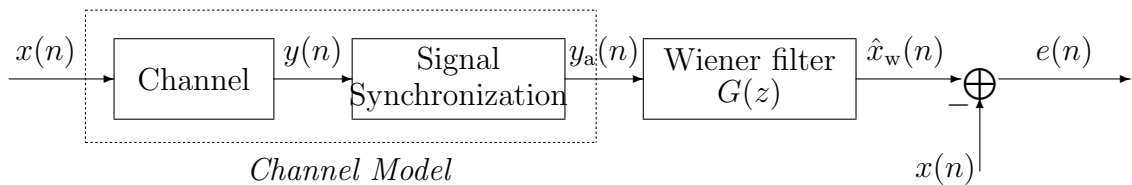


Figure 4.1: Block diagram of channel model and Wiener filter for signal estimation

We use a causal FIR Wiener filter $G(z) = \sum_{l=0}^{p-1} g(l)z^{-l}$. To design such a Wiener filter, define $x(n)$ as the desired signal, $y_a(n)$ as the observation signal. After pre-processing with removing delay, normalization and averaging, we assume that the received signal $y_a(n)$ is equal to the transmitted signal $x(n)$ with additive noise $w(n)$.

$$y_a(n) = x(n) + w(n) \quad (4.1.1)$$

Since the autocorrelation $r_{y_a}(k) = E\{y_a(n)y_a^*(n-k)\}$ and crosscorrelation $r_{xy_a}(k) = E\{x(n)y_a^*(n-k)\}$ are known, the desired signal $x(n)$ could be estimated from p observations samples from the previous time up to the current time. As described before, here since an expectation cannot be computed in reality, we estimated the correlation by summing.

In the design of a p -order causal FIR Wiener filter, the impulse response of the

filter is called $g(n)$. As $y_a(n)$ is the input to the filter, the output from Wiener filter $\hat{x}_w(n)$ is the convolution of $g(n)$ and $y_a(n)$,

$$\hat{x}_w(n) = g(n) * y_a(n) = \sum_{l=0}^{p-1} g(l)y_a(n-l) \quad (4.1.2)$$

Under the mean square error (MSE) criterion

$$\xi = E\{|e(n)|^2\} = E\{|x(n) - \hat{x}_w(n)|^2\} \quad (4.1.3)$$

the problem of Wiener filter is to find out the filter coefficients $g(k)$ that minimize the MSE,

$$\frac{\partial \xi}{\partial g^*(k)} = 0 \quad (4.1.4)$$

then Wiener-Hopf equations for Wiener filter is obtained [2]

$$\sum_{l=0}^{p-1} g(l)r_{y_a}(k-l) = r_{xy_a}(k), \quad k = 0, 1, \dots, p-1 \quad (4.1.5)$$

This is equivalent to the equation below

$$\begin{bmatrix} r_{y_a}(0) & r_{y_a}^*(1) & \cdots & r_{y_a}^*(p-1) \\ r_{y_a}(1) & r_{y_a}(0) & \cdots & r_{y_a}^*(p-2) \\ \vdots & \vdots & \ddots & \vdots \\ r_{y_a}(p-1) & r_{y_a}(p-2) & \cdots & r_{y_a}(0) \end{bmatrix} \begin{bmatrix} g(0) \\ g(1) \\ \vdots \\ g(p-1) \end{bmatrix} = \begin{bmatrix} r_{xy_a}(0) \\ r_{xy_a}(1) \\ \vdots \\ r_{xy_a}(p-1) \end{bmatrix} \quad (4.1.6)$$

since $y_a(n)$ is a complex value, here $r_{y_a}^*(k) = r_{y_a}(-k)$.

For simplicity, the equation above could be written as $\mathbf{R}_{y_a} \mathbf{g} = \mathbf{r}_{xy_a}$. Therefore the solution of optimal linear filter is obtained by the inversion of the autocorrelation matrix \mathbf{R}_{y_a} . Since \mathbf{R}_{y_a} and \mathbf{r}_{xy_a} are known, it is easy to find the coefficients of an optimal Wiener filter.

$$\mathbf{g}_{\text{opt}} = \mathbf{R}_{y_a}^{-1} \mathbf{r}_{xy_a} \quad (4.1.7)$$

The best estimation of the original signal $x(n)$ after a linear Wiener filter is

$$\hat{x}_{11}(n) = \hat{x}_w(n) = \sum_{l=0}^{p-1} g_{\text{opt}}(l)y_a(n-l) \quad (4.1.8)$$

As shown in Figure 4.2a, at -21 dBm, the resulting SNR from one complex Wiener filter normally reaches 40 dB when the filter length is longer than 5. Figure 4.2b illustrated that, when the input power is in linear phase between -30 dBm and 10 dBm, SNR remains stable around 40.6 dB. Here the Wiener filter length is chosen to be 20, which is long enough to obtain a satisfying SNR.

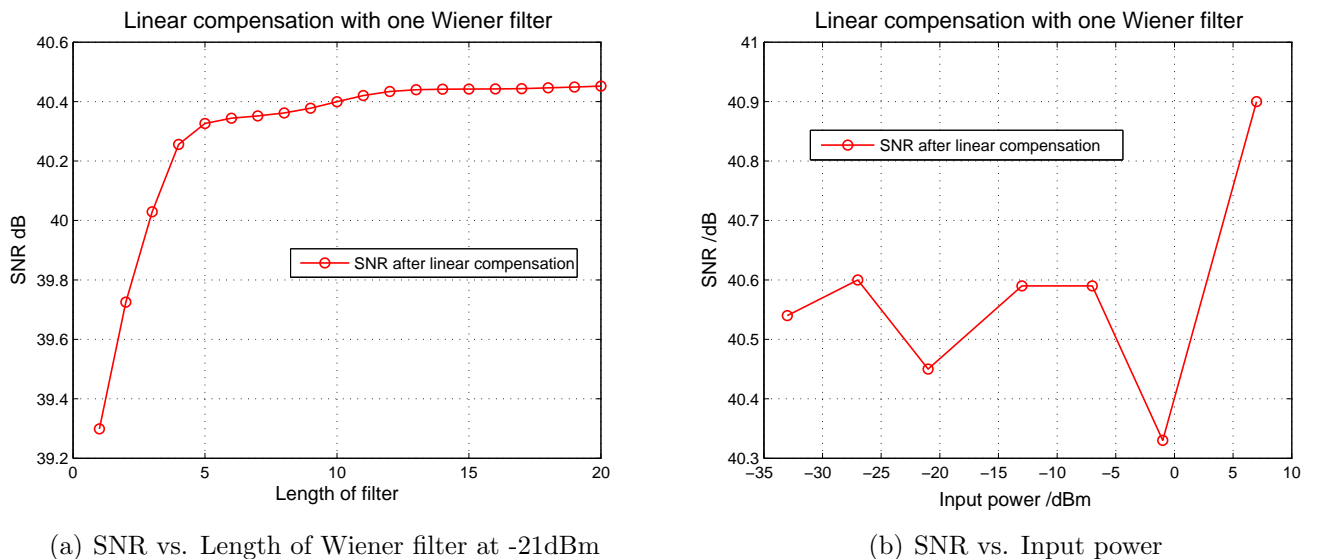


Figure 4.2: SNR after compensation by a complex Wiener filter

4.2 One Complex Channel Model and Imbalance Problem

In the previous section, we have assumed that the real part I and imaginary part Q of the signal are transmitted separately in the channel, without influence on each other.

Therefore, the crosstalk between I and Q were not considered when the Wiener filter had been designed.

However, as the analog modulator is non-ideal, there is an imbalance problem between I and Q part in the received signal. To model this problem, we establish an imbalance model between $x(n)$ and $\hat{x}_w(n)$, and use an imbalance matrix to compensate it, as shown in Figure 4.3.

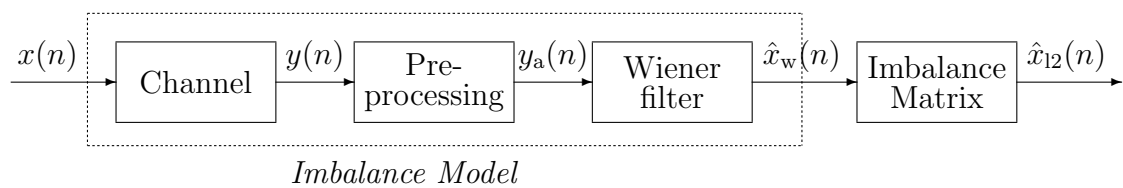


Figure 4.3: Block diagram of imbalance model and its compensation

By considering the cross effects, the imbalance model can be extracted in detail by four real constants filters h_{11} , h_{12} , h_{21} , h_{22} , shown in Figure 4.4. The filters coefficients can also be regarded as the gains between each two branches. [1]

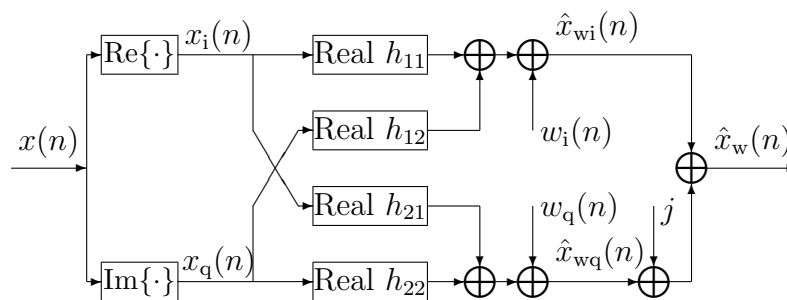


Figure 4.4: I/Q imbalance model

The output from Wiener filter $\hat{x}_w(n)$ can be described as

$$\begin{aligned}\hat{x}_w(n) = & \sum_{k=0}^{K-1} \{ [x_i(n-k)h_{11}(k) + x_q(n-k)h_{12}(k)] \\ & + j [x_i(n-k)h_{21}(k) + x_q(n-k)h_{22}(k)] \} \\ & + w_i(n) + jw_q(n)\end{aligned}\quad (4.2.1)$$

where $x(n) = x_i(n) + jx_q(n)$ is the baseband input signal, $w(n) = w_i(n) + jw_q(n)$ is the additive white noise. All four real filters have the same length K .

From the block diagram, h_{11} and h_{22} are the gain for original and estimated I and Q parts, which is expected to ideally equal to “1”; while h_{12} and h_{21} are cross gain between I and Q , which is expected to ideally equal to “0”. Then the relationship of original and estimated signal can be written in matrix form as:

$$\begin{bmatrix} \hat{x}_{wi}(n) \\ \hat{x}_{wq}(n) \end{bmatrix} = \begin{bmatrix} h_{11} & h_{12} \\ h_{21} & h_{22} \end{bmatrix} \begin{bmatrix} x_i(n) \\ x_q(n) \end{bmatrix}\quad (4.2.2)$$

As $x(n)$ and $\hat{x}_w(n)$ are the original signal and estimated signal from linear Wiener filter, which are already known, we can get a general solution for four real filter coefficients by transmitting several groups of signals in Equation 4.2.2.

$$\begin{bmatrix} h_{11} & h_{12} \\ h_{21} & h_{22} \end{bmatrix} = \begin{bmatrix} 0.9917 & 0.0012 \\ 0.0011 & 1.0078 \end{bmatrix}\quad (4.2.3)$$

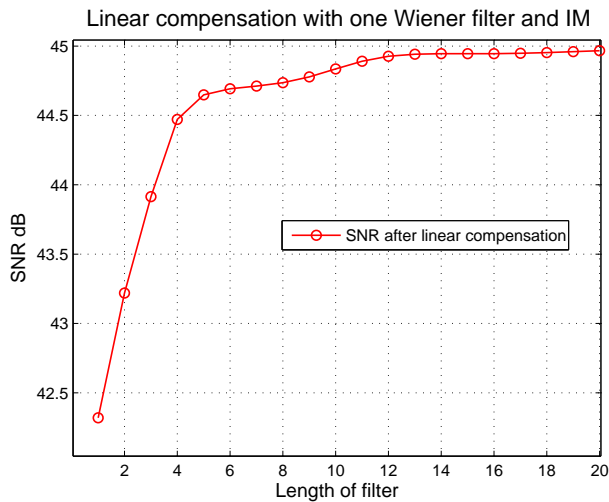
From measurements, it is obvious that I and Q channels are not completely independent. To compensate these imbalance effects, we just need to feed \hat{x}_w to the inverse of these four real filters. The imbalance matrix, therefore is

$$\begin{bmatrix} g_{11} & g_{12} \\ g_{21} & g_{22} \end{bmatrix} = \begin{bmatrix} h_{11} & h_{12} \\ h_{21} & h_{22} \end{bmatrix}^{-1} = \begin{bmatrix} 1.0084 & -0.0012 \\ -0.0011 & 0.9923 \end{bmatrix}\quad (4.2.4)$$

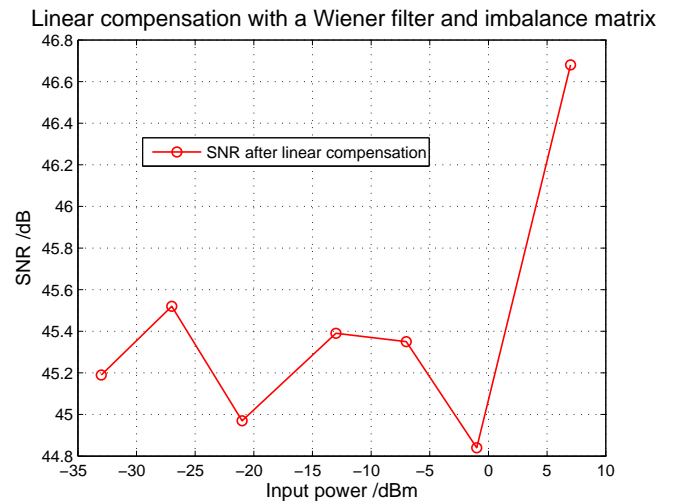
The output signal, which is called $\hat{x}_{12}(n)$, is the output from the whole linear compensation part including Wiener filter and imbalance matrix.

$$\begin{bmatrix} \hat{x}_{12i}(n) \\ \hat{x}_{12q}(n) \end{bmatrix} = \begin{bmatrix} g_{11} & g_{12} \\ g_{21} & g_{22} \end{bmatrix} \begin{bmatrix} \hat{x}_{wi}(n) \\ \hat{x}_{wq}(n) \end{bmatrix} \quad (4.2.5)$$

At -21 dBm transmitted power, the SNR after a complex Wiener filter and an imbalance matrix reaches to 45 dB, as illustrated in Figure 4.5a, the “IM” in the title of figure means the “imbalance matrix”. The imbalance matrix brings 5 dB improvement in SNR, comparing with compensating by just one Wiener filter. In Figure 4.5b, SNR remains stable around 45.5 dB between -30 dBm and 0 dBm.



(a) SNR vs. Length of Wiener filter at -21dBm



(b) SNR vs. Input power

Figure 4.5: SNR after compensation by a Wiener filter and imbalance matrix

4.3 Two Complex Channel Model and Two Wiener Filters

Since there is cross talk between I and Q channels, the channel can also be expressed by a two complex I/Q channel model, the corresponding compensation method also use two complex filters to compensate I and Q part respectively. Figure 4.6 shows a slightly rough block diagram of this procedure, and the detailed one will be extracted step by step.

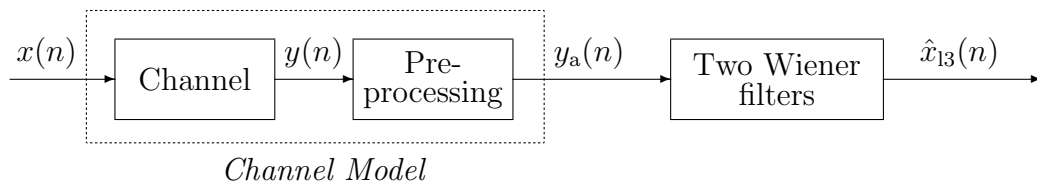


Figure 4.6: Block diagram of complex I/Q channel model and compensation

Here the input to the channel model is original signal $x(n)$, output is received signal $y_a(n)$, from equation 4.2.1, the relationship between them could be described as [1]

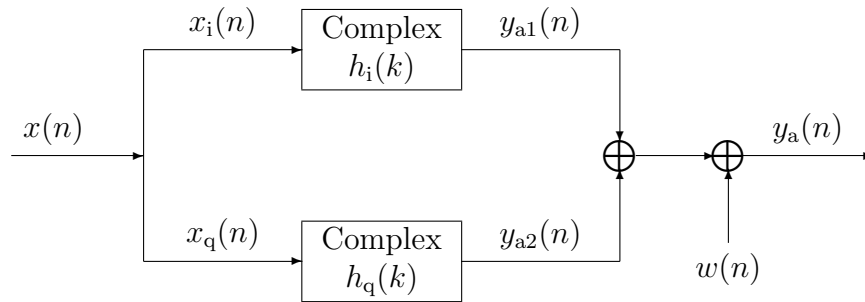
$$y_a(n) = \sum_{k=0}^{K-1} [x_i(n-k)h_i(k) + x_q(n-k)h_q(k)] + w(n) \quad (4.3.1)$$

the parameter K is the length of two filters h_i and h_q .

Then the channel model is illustrated in Figure 4.7.

In matrix form, it can be described as

$$\mathbf{y}_a = \mathbf{X}_i \mathbf{h}_i + \mathbf{X}_q \mathbf{h}_q + \mathbf{W} \quad (4.3.2)$$

Figure 4.7: Two complex I/Q channel models

where

$$\mathbf{X} = \begin{bmatrix} x(K-1) & x(K-2) & \cdots & x(0) \\ x(K) & x(K-1) & \cdots & x(1) \\ \vdots & \vdots & \ddots & \vdots \\ x(N-1) & x(N-2) & \cdots & x(N-K) \end{bmatrix}; \quad \mathbf{y}_a = \begin{bmatrix} y_a(K-1) \\ y_a(K-2) \\ \vdots \\ y_a(N-1) \end{bmatrix} \quad (4.3.3)$$

N is the length of $y_a(n)$.

Under the Least Square Error (LSE) criterion, we could find the channel coefficients. Define a cost function [1]:

$$\mathbf{J} = \|\mathbf{y}_a - \mathbf{X}_i \mathbf{h}_i - \mathbf{X}_q \mathbf{h}_q\|^2 \quad (4.3.4)$$

The optimal \mathbf{h}_i and \mathbf{h}_q that minimize the cost function can be found by setting the derivatives to 0,

$$\begin{aligned} \frac{\partial \mathbf{J}}{\partial \mathbf{h}_i^*} &= \mathbf{X}_i^H (\mathbf{y}_a - \mathbf{X}_i \mathbf{h}_i - \mathbf{X}_q \mathbf{h}_q) = 0 \\ \frac{\partial \mathbf{J}}{\partial \mathbf{h}_q^*} &= \mathbf{X}_q^H (\mathbf{y}_a - \mathbf{X}_i \mathbf{h}_i - \mathbf{X}_q \mathbf{h}_q) = 0 \end{aligned} \quad (4.3.5)$$

then we get

$$\begin{bmatrix} \mathbf{X}_i^T \mathbf{X}_i & \mathbf{X}_i^T \mathbf{X}_q \\ \mathbf{X}_q^T \mathbf{X}_i & \mathbf{X}_q^T \mathbf{X}_q \end{bmatrix} \begin{bmatrix} \mathbf{h}_i \\ \mathbf{h}_q \end{bmatrix} = \begin{bmatrix} \mathbf{X}_i^T \mathbf{y}_a \\ \mathbf{X}_q^T \mathbf{y}_a \end{bmatrix} \quad (4.3.6)$$

Therefore, the coefficients for the two complex channels are

$$\begin{bmatrix} \mathbf{h}_i \\ \mathbf{h}_q \end{bmatrix} = \begin{bmatrix} \mathbf{X}_i^T \mathbf{X}_i + \sigma^2 \mathbf{I} & \mathbf{X}_i^T \mathbf{X}_q \\ \mathbf{X}_q^T \mathbf{X}_i & \mathbf{X}_q^T \mathbf{X}_q + \sigma^2 \mathbf{I} \end{bmatrix}^{-1} \begin{bmatrix} \mathbf{X}_i^T \mathbf{y}_a + \sigma^2 \mathbf{e} \\ \mathbf{X}_q^T \mathbf{y}_a + j\sigma^2 \mathbf{e} \end{bmatrix} \quad (4.3.7)$$

where σ^2 is the variance of artificial white noise, \mathbf{I} is a $K \times K$ identity matrix, and $\mathbf{e} = [1 \ 0_{K-1}^T]$, 0_{K-1} is length $K - 1$ column vectors filled with zeros. Such diagonal loading is introduced to improve the numerical properties of the matrix inverse.

To construct the I/Q compensator, we just need to inverse the channel model above, so the two complex compensation filters \mathbf{g}_i and \mathbf{g}_q are

$$\begin{bmatrix} \mathbf{g}_i \\ \mathbf{g}_q \end{bmatrix} = \begin{bmatrix} \mathbf{Y}_{ai}^T \mathbf{Y}_{ai} + \sigma^2 \mathbf{I} & \mathbf{Y}_{ai}^T \mathbf{Y}_{aq} \\ \mathbf{Y}_{aq}^T \mathbf{Y}_{ai} & \mathbf{Y}_{aq}^T \mathbf{Y}_{aq} + \sigma^2 \mathbf{I} \end{bmatrix}^{-1} \begin{bmatrix} \mathbf{Y}_{ai}^T \mathbf{x} + \sigma^2 \mathbf{e} \\ \mathbf{Y}_{aq}^T \mathbf{x} + j\sigma^2 \mathbf{e} \end{bmatrix} \quad (4.3.8)$$

Figure 4.8 shows the detailed structure of channel model and two complex filters for I/Q compensation.

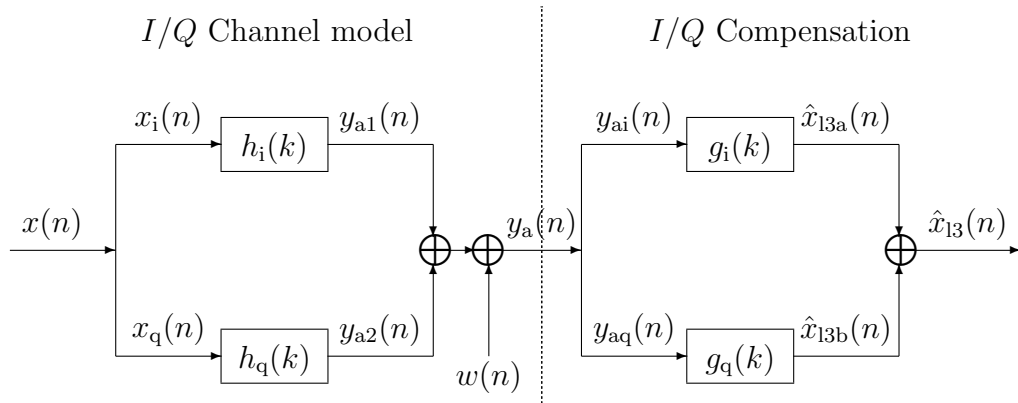


Figure 4.8: Detailed two complex I/Q channel model and compensation

The best estimation of original signal $x(n)$ by two complex linear filters therefore is

$$\hat{x}_{13}(n) = \sum_{k=0}^{K-1} [y_{ai}(n-k)g_i(k) + y_{aq}(n-k)g_q(k)] \quad (4.3.9)$$

The third linear compensation method use two complex filters under least square error criterion to replace the second one which uses one complex Wiener filter and a imbalance matrix. In our experiment, both of these two methods brought a significant improvement in SNR, reaching 45 dB. But in a real implementation, the third method with two complex filters is more feasible, since the coefficients of the imbalance matrix is changable depend on different modulators.

As displayed in Figure 4.9a, the SNRs after two complex filters are over 45.2 dB at -21 dBm. Without imbalance matrix, the imbalance problem still could be solved by two complex compensation filters. In Figure 4.9b, SNRs are around 45.7 dB between -30 dBm and 0 dBm.

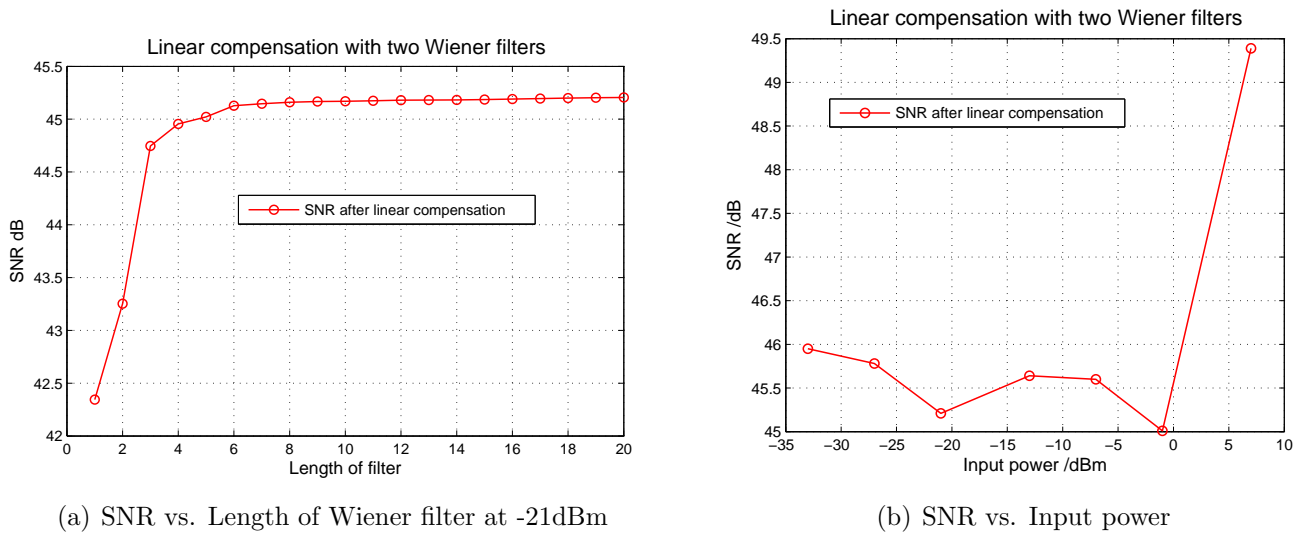


Figure 4.9: SNR after compensation by two complex Wiener filters

4.4 Measurement Results Comparison

The measurement results for the above three linear compensation methods are summarized in this section. In this process, the input to the linear compensation filters is the pre-processed complex signals $y_a(n)$; the output $\hat{x}_1(n)$ is the best linear estimation of the original signal $x(n)$ under MSE or LSE criterion.

We measured the final Signal-to-Noise Ratio (SNR) between $x(n)$ and $\hat{x}_1(n)$ in dB with compensation filters' length from 1 up to 20. Figure 4.10 and Table 4.1 below shows the measurement results in SNR when the input power is -21 dBm, by using the three compensation methods presented in this chapter.

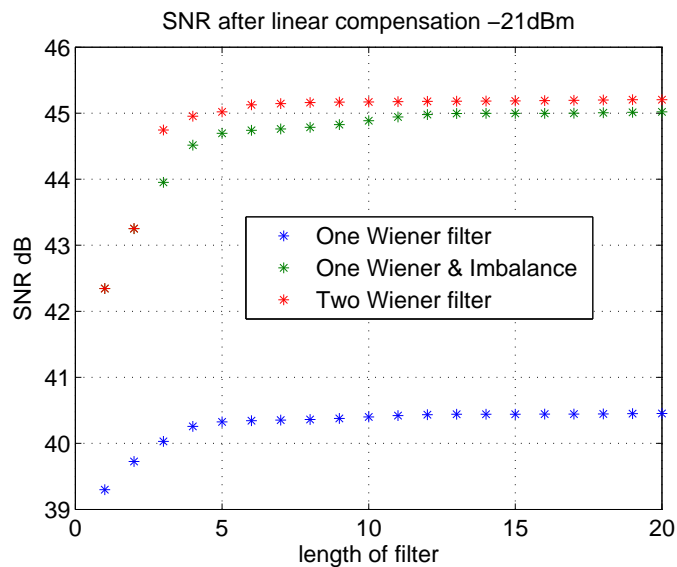


Figure 4.10: SNR vs. Length of filters after linear compensation at -21 dBm

As shown in Figure 4.10, all three curves tend to be stable with filter length longer than 5, reaching a plateau at 40.5 dB, 45 dB and 45.2 dB for the three methods respectively. Since the SNR after averaging is around 39.2 dB, the best linear

Table 4.1: SNR comparison when input power is -21 dBm

Power = -21 dBm	SNR
<i>Before averaging</i>	35 dB
<i>After averaging</i>	39.2 dB
<i>One Wiener filter</i>	40.5 dB
<i>One Wiener filter with Imbalance matrix</i>	45 dB
<i>Two Complex filters</i>	45.2 dB

compensation method by two complex filters could improve SNR up to 6 dB.

It is also obvious that SNR increases 4.5 dB after compensating the I/Q imbalance problem in the modulator, which is an indispensable improvement. Therefore, although the imbalance effect between I and Q channels seems small, it needs to be compensated for.

For different input power, the measurement result in SNR is shown in Figure 4.11.

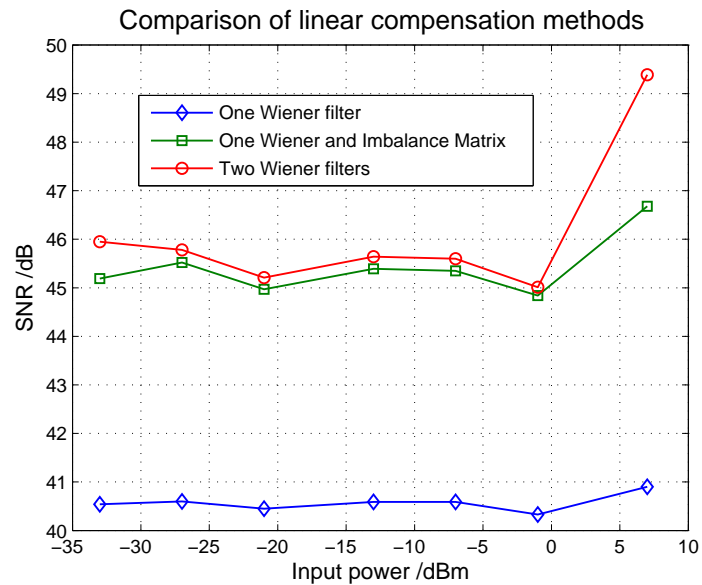


Figure 4.11: SNR vs. Input power after linear compensation

From -30 dBm to 0 dBm, the SNRs remain stable around 40.6 dB, 45.5 dB and 45.7 dB for the three methods respectively. Therefore, in this range of input power, the compensation methods we introduced in this section could bring satisfying progress in SNR. But when the input power is below -35 dBm or above 5 dBm, the SNR changed dramatically, which is caused by the hardware limitation of ESG and OSC. The OSC could not detect the signals below -35 dBm and the ESG could not linearly amplify the signals above 5 dBm, therefore the results are abnormal and unreliable. In our opinion, maybe it is because that the compensation parameters are derived when the input power is 7dBm, which reflects the characteristics of this channel. Therefore, this group of parameters performs better on this channel than the rest of channels.

Chapter 5

Modeling and Compensating for Nonlinear Distortion

Generally, every electric equipment has a nonlinear transfer characteristics. The nonlinearities might cause the residual error contributions to the whole system, for instance, out of band distortion, instability of power amplifiers, different phase shift according to different frequencies, etc. This distortion could not be solved by linear compensation, like Wiener filters, thus, nonlinear compensation is the key to solve the problems.

5.1 Identification of Nonlinear Effects

Getting to know how nonlinear the system is, a common method is used to compare the power of the output signal with the desired output power. In a linear system, the power of output signals should be equal to the desired setups. However, in a non-ideal system, especially with high transmitted powers, the output power could not change according to the power setup relevantly. Therefore, the system like this is judged to be nonlinear system. This method is used in our test to estimate whether

the system is linear or not. The comparison of the output power and the desired setup is presented in Figure 5.1.

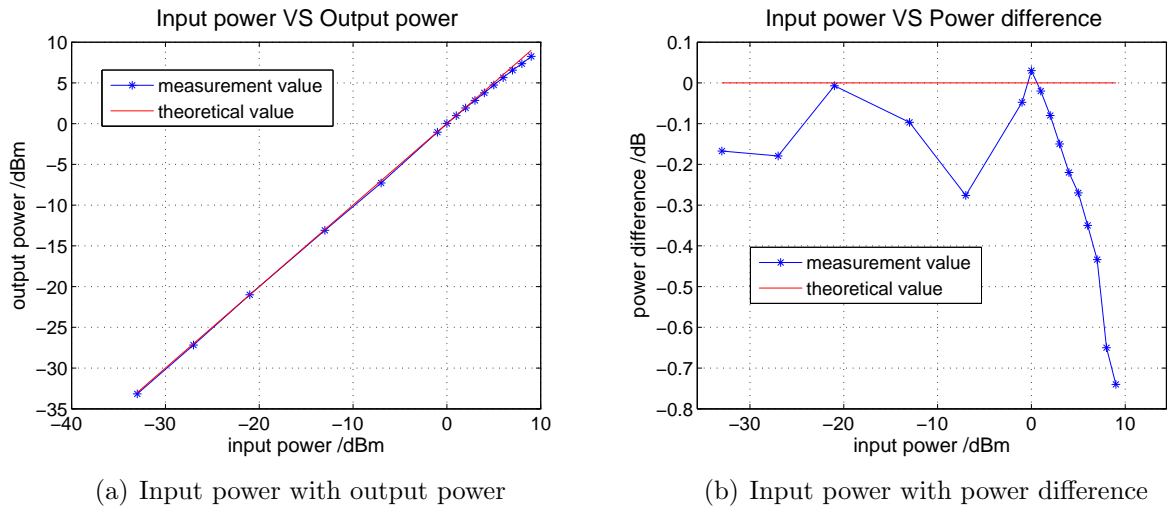


Figure 5.1: Theoretical and measured power comparison for the input and output signal.

In Figure 5.1(a), the red line is set to be a reference, meaning that the output power is equal to the setup. A system which could fulfill this situation is a linear system. While, the blue stars are from the measurement data. The blue curve is bend at high power range. Figure 5.1(b) presents the power difference between the setup and output signals. The higher power we set, the more obvious the power gap is. Therefore, this measurement system has the characteristic of nonlinearity.

5.2 Nonlinear Model

Since we are analyzing the I/Q modulation system, first, let us take a look at the components that might cause nonlinear problems. The Figure 5.2 presents the dominating nonlinear components, in dashed boxes.

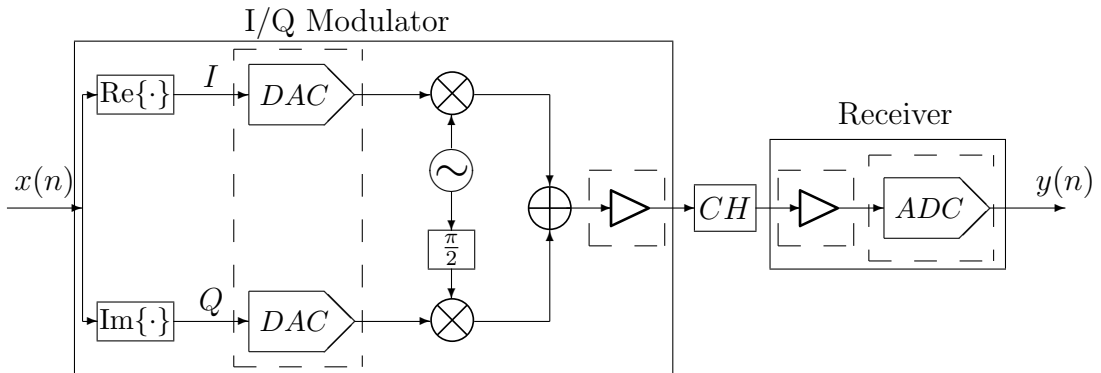


Figure 5.2: Nonlinear components within the system model

From Figure 5.2, the two D/A converters and the first amplifier belongs to I/Q modulator, while the second power amplifier and the A/D converter are inside the receiver. Since only the input and output signals could be measured, the whole system is unified and analyzed as one nonlinear model.

Nonlinear models are categorized into several types by their properties, for instance, the memory and memoryless models, the AM/AM and AM/PM models, the basepass and bandpass models, etc. [3] When compensating the system, the compensation methods should be corresponding to which system model is used.

5.2.1 Memory and memoryless model

The nonlinear system could be described by a memoryless model when the output signal is only depending on the input at the same time point. It could be presented as

$$y(n) = L\{x(n)\} \quad (5.2.1)$$

where x is the input signal, y is the output signal, see Figure 5.2. $L\{\bullet\}$ is the nonlinear function.

The $p + q^{\text{th}}$ order memory nonlinear model is

$$y(n) = \sum_{k=n-p}^{n+q} L\{x(k)\} \quad (5.2.2)$$

the system is causal when $q = 0$.

5.2.2 AM/AM and AM/PM model

A nonlinear system is generally a combination of the AM/AM model and AM/PM models (AM: Amplitude Modulation; PM: Phase Modulation). AM/AM model adjusts the output signal's amplitude based on the input signal. AM/PM model varies the signal phase based on the input signal amplitude. Figure 5.3 illustrates the nonlinear model including both AM/AM and AM/PM [3].

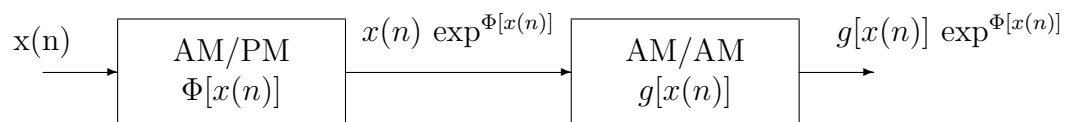


Figure 5.3: Block model for AM/AM and AM/PM envelope nonlinearity

where $\Phi[x(n)]$ and $g[x(n)]$ are the two nonlinear functions needed to be solved out.

$$y(n) = g[x(n)] \exp^{\Phi[x(n)]} \quad (5.2.3)$$

With a narrow band input signal, the phase shift caused by the nonlinear system could be ignored. Using polynomial to represent the AM function,

$$y(n) = g[x(n)] = \sum_{i=0}^P a_i |x(n)|^i \quad (5.2.4)$$

where P is the order of the polynomial. This harmonic is going to be used to treat the measurements.

The baseband and passband nonlinear models are classified by the characteristic of the frequency response of the system, whether it is baseband system or the passband system.

5.3 Nonlinear Compensation

Since the input signal $x(n)$ is a 8 MHz baseband white noise, in our case study, it is seen as a narrow band signal compared to the carrier frequency $f_c = 2.14$ GHz. An AM/AM model is utilized as the system model. Also, the inner signal interference has been eliminated by Wiener filter during the linear compensation, so the nonlinear model is set to be memoryless. The block diagram of the nonlinear compensation is presented as in Figure 5.4. $\hat{x}_1(n)$ is the output signal from the linear compensation,

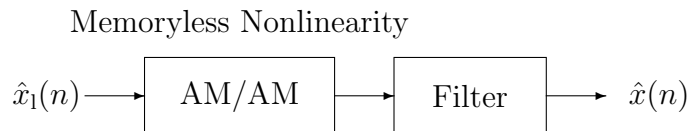


Figure 5.4: Simplified One Nonlinearity–One Filter (Two-Box) Model

while $\hat{x}(n)$ is the output signal from the nonlinear compensation.

Given the channel model as Figure 5.4, Equation 5.3.1 as below is the mathematical model,

$$|\hat{x}(n)| = \sum_{i=0}^P a_i |\hat{x}_1(n)|^i \quad (5.3.1)$$

where P is the maximum order of the polynomial. The larger P is, the more accurate the polynomial model is, though it brings more calculation complexity. Moreover, when the order of polynomial is too large, its performance will decrease because of numerical problems. P is supposed to be a small number providing good performance. While, the phases keep the same.

The Equation 5.3.1 could be extended as:

$$\begin{bmatrix} |\hat{x}(1)| \\ |\hat{x}(2)| \\ \vdots \\ |\hat{x}(N)| \end{bmatrix} = \begin{bmatrix} |\hat{x}_1(1)| & |\hat{x}_1(1)|^2 & \cdots & |\hat{x}_1(1)|^P \\ |\hat{x}_1(2)| & |\hat{x}_1(2)|^2 & \cdots & |\hat{x}_1(2)|^P \\ \vdots & \vdots & \ddots & \vdots \\ |\hat{x}_1(N)| & |\hat{x}_1(N)|^2 & \cdots & |\hat{x}_1(N)|^P \end{bmatrix} \begin{bmatrix} a_1 \\ a_2 \\ \vdots \\ a_P \end{bmatrix} \quad (5.3.2)$$

where N is the length of the signal.

Here a_i don't have to be calculated for different input powers. Instead, polynomial parameters derived from the highest input power cover the nonlinear characteristics of the system. In our experiments, the input power $p = 7$ dBm is the highest power, which is utilized to extract the system parameters.

After calculating the a_i , the estimation of $x(n)$, which is named $\hat{x}(n)$ could be derived from Formula 5.3.1.

5.4 Measurement Results

Using Formula 5.3.2, a_i is calculated from the highest input power $p = 7$ dBm, which causes the most nonlinear situation. Figure 5.5 presents the SNR's improvement with increasing polynomial order. From the figure below, order 5 is enough to obtain a satisfying SNR.

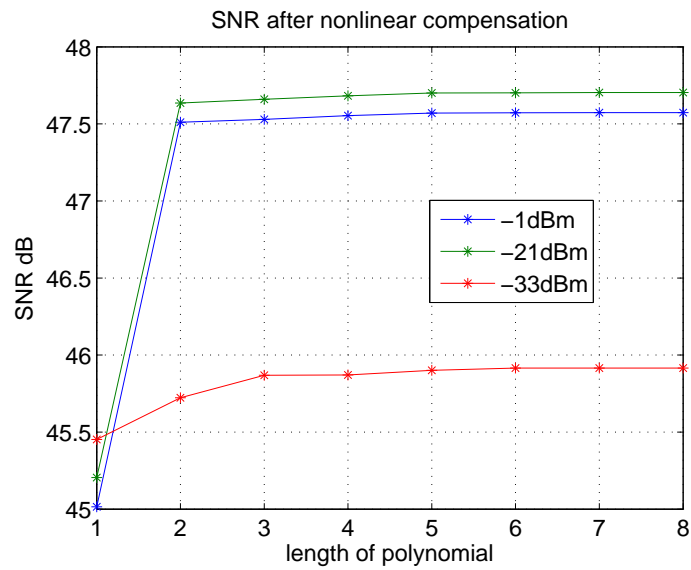


Figure 5.5: SNR after nonlinear compensation with different orders and signal power

The SNRs derived from different input powers are shown in Figure 5.6. The enhancements of SNRs after nonlinear compensation are from 1 dB to 2.5 dB. In some cases, for instance, $p = -33$ dBm and $p = -13$ dBm, the nonlinear compensation only improves the SNR by 1 dB, while with some other input powers, $p = -21$ dBm and $p = -1$ dBm, SNR improves by 2.5 dB. In despite of the different gain, all the SNRs achieve to 46.5 dB.

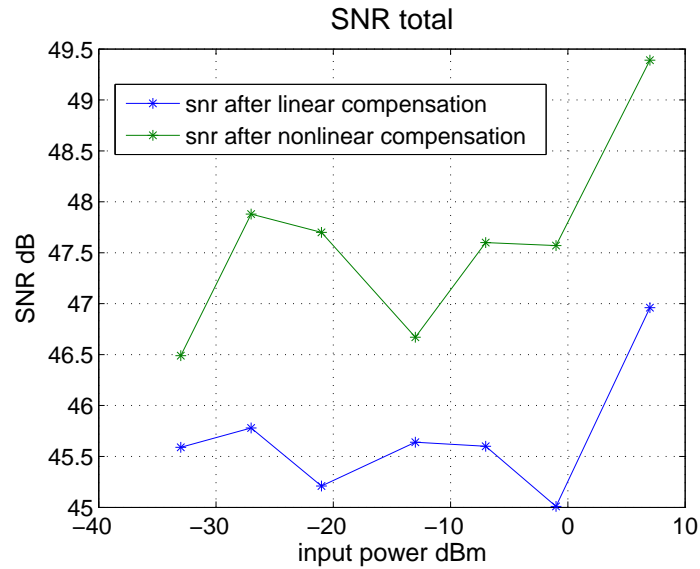


Figure 5.6: SNR before and after nonlinear compensation

5.4.1 Discussion on OSC's scaling setup

As mentioned in Chapter 2, the scaling setting of the OSC is always changing according to different input powers. This makes the receiver works always in the proper situations. However, every time that we change the scaling, the OSC is switched to a new physical channel. The characteristic for every channel could be eliminated only if there is a separate model for each scaling setting. Since the nonlinear model is derived from $p = 7$ dBm and set to be the uniform model, it can not cover all the individual aspects. Therefore, the performance of the compensation method could not work equally well for every case.

Another experiment is designed to demonstrate how much the scaling setting affects the quality of the compensation. With a fixed input power $p = 5$ dBm, a signal is transmitted three times with different scaling settings on the OSC, which are 100mV/, 200mV/ and 500mV/. Figure 5.7 illustrates the OSC's view of those

three measurements.

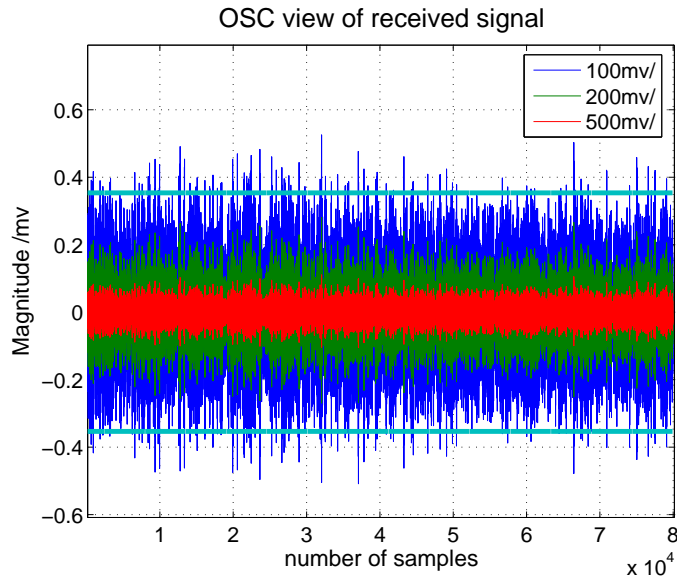


Figure 5.7: The OSC view of the received signal with input power $p = -5\text{dBm}$, three scaling settings.

The two thick light-blue lines are the upper and lower edges of the OSC's monitor. The signals between them are the visible portion. The SNR of those three received signals are exhibited in Table 5.1. The most appropriate scaling is 200mV/, which leads to the highest SNR=47.5 dB. While, the SNR with rest two scalings are 4 dB lower.

Table 5.1: Signal performances according to scaling

<i>Scaling</i> mV/	100	200	500
<i>SNR</i> dB	43.2	47.5	43

So far, the whole measurement system model identification has been done. The characteristics of this model are used for compensating it in the next chapter.

Chapter 6

Pre-compensation

In this chapter, previous parameters derived from channel modeling are used to compensate the signal before it is sent to the transmitter. The experiment of pre-compensation follows the procedure of Figure 6.1.

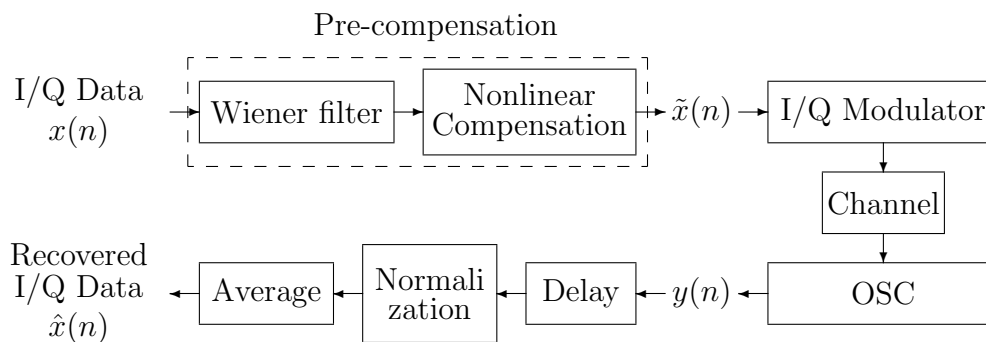


Figure 6.1: Pre-compensation Progress

In the figure, $\tilde{x}(n)$ is the pre-compensated baseband bandlimited signal that is sent to I/Q modulator. $y(n)$ is received from OSC and goes to the measurement improvement blocks. Except for a time delay and amplitude offset, this signal should

correspond to $x(n)$. In order to compare $y(n)$ to the input data, it needs to be delay compensated and normalized as described in Chapter 2. At last, $\hat{x}(n)$ is used to evaluate the representation of the whole system.

Since the parameters of Wiener filter are derived from sample frequency $f_{osc} = 200\text{MHz}$, while $x(n)$ is sampled at $f_s = 50\text{MHz}$, the Wiener filter can not be used to filter $x(n)$ directly. In this way, $x(n)$ could be resampled to 200 MHz, or instead, Wiener filter could be recomputed to correspond to 50 MHz. Here for simplicity, we chose the previous method. Having been filtered by the Wiener filter, the signal is downsampled back to f_s and transmitted to the nonlinear compensation block. Besides, downsampling could be located after the polynomial as well, which performs equally good while causing four times amount of calculation though.

Figure 6.2 presents the SNR comparison of with and without pre-compensation. The pre-compensated signal regardless of the input power could bring more than 4 dB SNR improvement.

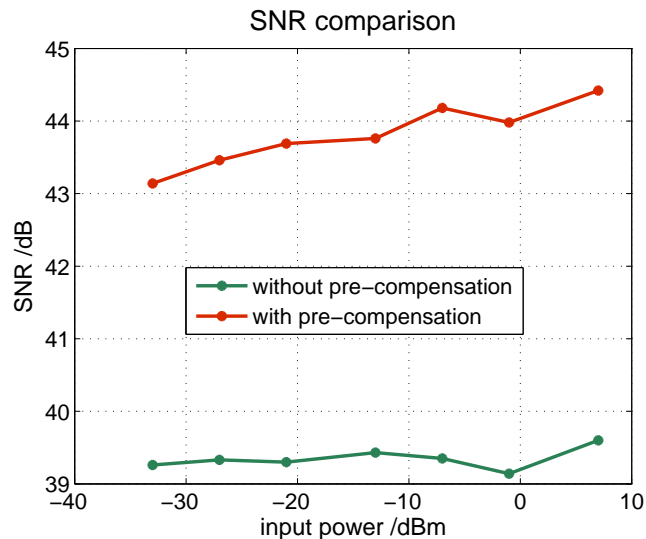


Figure 6.2: SNR with and without precompensation

As a conclusion, following the procedure we did in this project, the measurement results for each step is illustrated in Figure 6.3. The post-compensation, including averaging, linear and nonlinear compensation, brings approximate 13 dB improvement in SNR, while pre-compensation brings 9 dB. We lose 4 dB in pre-compensation, but it is technically inevitable, because the coefficients for compensation, which were obtained from a group of training signals, are not perfectly fitted for any other random signals.

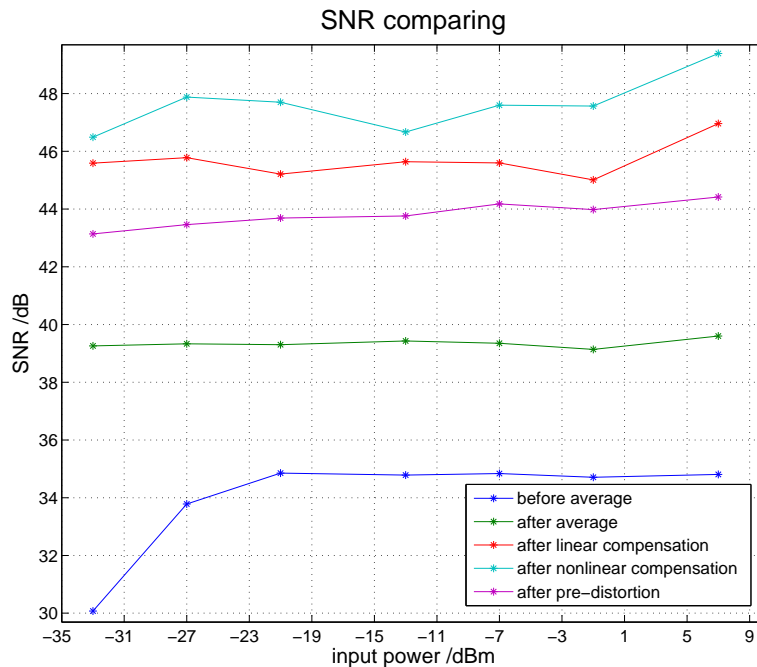


Figure 6.3: SNR comparison

For the blue curve that shows the SNRs before averaging, the SNRs are low when the input power is below 21 dBm, because the noise dominated low power signals and therefore reduced the SNRs. What is also worthy of being mentioned is that, the results will have slight difference according to each scaling setting.

Chapter 7

Conclusion

In this thesis work, by considering the non-ideal property of the I/Q modulator, an extensive model has been developed from measurements. The model includes linear and nonlinear compensation and has been identified using various synchronization and DSP techniques.

Firstly the received signal is synchronized and optimized by removing accurate delay, averaging and normalizing. After that, we extracted the accurate I/Q modulator model, emphasizing on solving the imbalance problem between I and Q channels and the modulator's nonlinearity. The model is then used to find linear Wiener filter and nonlinear polynomial estimation for the post-compensation. When the filters' coefficients were obtained, pre-compensation is applied. In communication field, pre-compensate is more reasonable and feasible to be used.

After these efforts, a significant improvement in SNR was achieved, the results are illustrated in Figure 6.3. Generally, preprocessing gives 4.5 dB improvement, linear and nonlinear compensation bring 6 dB and 2.5 dB respectively, so the total improvement after post-compensation is around 13 dB in SNR, from 35 dB to 48 dB. As the final utilization, pre-compensation could provide 9 dB improvement, from 35

dB to 44 dB.

For the further research, the compensation for the non-ideal I/Q modulator could be extended for wireless transmission. As the channel is different from wired transmission, new distortions will be introduced and new compensation methods will be applied for the signals.

Bibliography

- [1] L. Ding, Z. Ma, D. R. Morgan, M. Zierdt, and G. T. Zhou, *Frequency-dependent modulator imbalance in predistortion linearization systems: Modeling and compensation*, IEEE (2003), 688–691.
- [2] Monson H. Hayes, *Statistical digital signal processing and modeling*, John Wiley, New York, USA, 1996.
- [3] Philip Balaban Michel C. Jeruchim and K. Sam Shanmugan, *Simulation of communication systems: Modeling, methodology, and techniques*, Kluwer Academic/Plenum Publishers, 233 Apring Street, New York, N.Y. 10013, 2000.
- [4] Richard Quinnell, *Designing digital filters*, TechOnline <http://www.dspdesignline.com/showArticle.jhtml?articleID=192200504> (2003).
- [5] Neil L. Scott Rodney G. Vaughan and D. Rod White, *The theory of bandpass sampling*, IEEE TRANSACTIONS ON SIGNAL PROCESSING. VOL. 39. NO. 9 (1991).